

BEXYL
BEYOND XYLELLA

Discovery of functional peptides, antimicrobial glass ceramics and plant extracts and bacteriophages against *Xylella fastidiosa*

Deliverable 6.2

31 May 2025

Author(s): Emilio Montesinos (P4-UdG); Blanca B. Landa, Miguel Román, Juan A. Navas Cortés (P1-CSIC-IAS); Pilar Domingo-Calap (P1-CSIC-UV-I2SysBio); Ester Marco-Noales, Carlos Sellés Ribera (P2-IVIA).

Funded by the European Union

DELIVERABLE INFORMATION

Start of the project:	01 Sep 2022
Duration:	48 months
Coordinator:	Blanca B. Landa
Deliverable title:	Discovery of functional peptides, antimicrobial glass ceramics and plant extracts and bacteriophages against Xf.
Deliverable n°:	D6.2
Nature of the deliverable:	Report
Dissemination level:	Sensitive
WP contributing:	WP6
Lead beneficiary:	University of Girona (P4-UdG)
Due date of deliverable:	31 May 2025
Actual submission date:	30 May 2025

Deliverable status

Ver.	Status	Date	Author(s)
1.0	Final	30 May 2025	Emilio Montesinos (P4-UdG); Blanca B. Landa, Miguel Román, Juan A. Navas Cortés (P1-CSIC-IAS); Pilar Domingo-Calap (P1-CSIC-UV-I2SysBio); Ester Marco-Noales, Carlos Sellés Ribera (P2-IVIA)

Disclaimer

The content of this deliverable does not necessarily reflect the official opinions of the European Commission or other institutions of the European Union.

Funded by the European Union

Table of contents

ABSTRACT 4

1. Introduction 6

2. METHODOLOGY AND RESULTS 9

2.1. Vitocristaline glasses and glass-ceramics 9

2.1.1. Antimicrobial activity of glasses and glass-ceramics 9

2.1.2. Phytotoxic activity of glasses and glass-ceramics 15

2.2. Plant extracts 17

2.2.1. Antimicrobial activity of extracts from 'alperujo' 17

2.2.2. Eucalyptus essential oil 23

2.3. Peptides 25

2.3.1. Activity of single peptides 25

2.3.2. Screening *in planta* of selected single peptides 31

2.3.2.1. *Nicotinana benthamiana* as a model to screen peptides against *X. fastidiosa* 33

2.3.2.2. Screening of peptides in almond (*Prunus dulcis*) 35

2.3.3. Screening of random peptide mixtures 42

2.4. Bacteriophages 43

2.4.1. Characterization of a collection of phages 43

2.4.2. Phage host range 48

2.4.3. Screening *in planta* of selected bacteriophages 49

3. CONCLUSIONS 51

4. Publications from this deliverable 52

4.1. Articles published 52

4.2. Articles in preparation or under revision 52

5. REFERENCES 53

Funded by the European Union

ABSTRACT

Chemical control has been the dominant approach for the control of *X. fastidiosa* diseases focused on the control of its insect vectors, but there is no practical cure for *X. fastidiosa* under field conditions once a plant become infected. In this deliverable D6.2, entitled "**Discovery of functional peptides, antimicrobial glass ceramics and plant extracts and bacteriophages against *Xylella fastidiosa***" we present the results gathered on WP6 focused on developing and evaluating novel environmentally-friendly compounds for control of this bacterium.

The highest bactericidal effect of the **antimicrobial glasses and glass-ceramics** obtained by the CSIC was found for the GT3 glass, and the other compounds (G3 and CIN) required several hours of treatment to show some efficacy. Short treatment times did not affect bacterial cell viability.

Three types of **antimicrobial glass materials**—G3, CIN, and G3T—were evaluated for their bactericidal activity against multiple *X. fastidiosa* subspecies and sequence types. G3T, a vitrocrystalline glass obtained through optimized thermal treatment, demonstrated the highest bactericidal efficacy, achieving full suppression of colony formation after 48 hours of exposure for most strains. Bacterial viability, measured through v-qPCR, also confirmed the time-dependent cytotoxicity of the glass formulations, with G3T consistently reducing viable cells to below 5%. Phytotoxicity tests on *Nicotiana benthamiana* leaves indicated some toxicity, especially at higher concentrations, which must be accounted for in formulation development.

A range of phenolic-rich **plant extracts derived from olive oil by-products (*alperujo*)** were tested, including hydroxytyrosol (HT), DHFG, HT-DHFG, digestate and R1. HT exhibited the most potent and rapid bactericidal activity, impairing colony development within 1 hour at concentrations as low as 2%. However, HT was also the most phytotoxic. Other extracts such as R1 and HT-DHFG offered a balance between antibacterial efficacy and lower phytotoxicity. Additionally, eucalyptus essential oil (EGL2 formulation) showed rapid bactericidal activity through membrane lysis and reduced disease severity in almond plants via both bactericidal and plant defense-inducing effects, without observed phytotoxicity in planta.

The most active **synthetic single peptides** on growth inhibition and bactericidal activity against most of the STs were BP178, 1036 and BP473. As expected, Peps did not show any effect on the culturability or bactericidal activity. The peptide with the broadest antibiofilm activity against the selected STs was BP178 but did not show antibiofilm activity against ST53. It is interesting to note that peptides 1036 and BP473 presented high antibiofilm activity against ST53, which is of special relevance since it's the causal agent of Olive Quick Decline Syndrome. *Nicotiana benthamiana* and almond plants (cv. Avijor) were used to test the effect of selected peptides in plant response by following the expression levels of defence-related genes in leaves. The peptides that showed better results in the overexpression of defence genes were BP178 and HH15. Additionally, the BP178 peptide presented the ability to upregulate several genes such as ERF1 (Ethylene transcription factor), LOX (Lypoxygenase), PR1 (pathogenesis-related genes) PR3 (Endochitinase) and PR2 (Glucanase) all of them involved in signalling by pathogen attack by salicylic acid pathway, MAPK3 (Mitogen-activated protein kinase 3) which play a central role in PAMP-triggered immunity. Another peptide that

Funded by the European Union

stood out was HH15, showing high overexpression of all PR genes (PR3, PR1, PR2, PR4a and PR4a, pathogenesis-related genes). The HH15 peptide showed overexpression results well above the BP178 peptide, showing itself as a very good candidate to achieve the objective of obtaining *priming* plants. Also, the peptides BP473, FV7 and 1036 showed overexpression in some of the genes analysed (LOX, PAL, WRKY25, WRKY22, and MAPK3) and controlled significantly *X. fastidiosa* infection in several subspecies and STs. The activity of random peptide mixtures (RPMs) was confirmed by optical density measurements in growth media, but the CFU count results were inconsistent and no conclusions could be reached.

An important collection of **bacteriophages**, isolated from wastewater plants in Valencia (Spain) has been generated. After their characterization, 19 new virulent phages with high in vitro lytic activity against different European strains of *X. fastidiosa* subsp. *fastidiosa*, belonging to the genus Pradovirus (9), Alphatectivirus (6), Bosavirus (1), Salvovirus (1) and 2 unclassified within Autographiviridae family have been selected. Moreover, greenhouse experiments with one selected phage, vB_Xf_IVIA-DOCa19P19, showed a clear inhibitory effect in planta (periwinkle and tobacco) both in preventive and therapeutic treatments. *X. fastidiosa* could not be isolated from most of the phage-treated infected plants and could not even be detected by PCR, this was correlated with high concentrations of phages as quantified by a phage-specific qPCR protocol designed in this framework of BeXyl, suggesting the biocontrol activity of the phage in planta. Finally, to further investigate the potential use of a selected phage in the field, a pilot study was conducted in Balearic Islands (Spain) in an area with an active outbreak of Pierce's disease in grapevines, and mitigation of PD symptoms was successful.

In summary, the results of this deliverable provide compelling evidence for the feasibility of using alternative, sustainable agents for the integrated management of *X. fastidiosa* in line with the EU Green Deal and Farm to Fork strategy. The combined efficacy of antimicrobial glass-ceramics, plant-based antimicrobials, functional peptides, and phage therapy offers a diversified toolbox with potential for future field application. Further work is needed to validate these findings under open field conditions and optimize formulations for regulatory approval and farmer adoption. Some of these activities will be conducted in the frame of WP7 and presented in deliverable D7.3.

Funded by
the European Union

1. INTRODUCTION

Since there is no practical cure for *X. fastidiosa* under field conditions, control strategies applied in the EU have been focused on: (1) **exclusion and eradication**, (2) **control of vectors;** (3) exploiting **hosts genetic natural resistance/tolerance**, (4) **agricultural practices** (pruning, cover crop management, etc.), and other methods focused to cure or minimize the disease in plants by the application of (5) **some chemical or biological treatments** (Figure 1) (EFSA PLH Panel, 2018, 2019). However, for Italy, the only country where those control practices have been tested so far, they appear to not be sufficient to stop the spread of the epidemic or mitigate disease severity, which highlights the need to find new approaches for the management of *X. fastidiosa* (Morelli et al., 2021; Burbank, 2022). Removal of infected trees and chemical insect vector control have a strong negative environmental and economic impact on agricultural ecosystems. Thus, management of *X. fastidiosa* diseases must be oriented to develop **effective and sustainable solutions** in line with the EU Green Deal and the Farm to Fork strategy (Tataridas et al., 2022; Marelli et al., 2025).

Chemical control has been the dominant approach for the control of *X. fastidiosa* diseased plants. The application of antibiotics such as oxytetracycline via trunk injections, spray or irrigation have provided reduction of disease symptoms. However, there is a need to repeat the treatment periodically, and antibiotic use in agriculture is currently forbidden within the EU territory (Amanifar et al., 2016). Several chemical compounds have been tested (including N-Acetylcysteine (NAC), an analogue of cysteine that affects biofilm formation (Bruno et al., 2021; Picchi et al., 2024); Fosetyl aluminum (Tatulli et al., 2024); Harpin protein; COS-OGA; and Acibenzolar S-methyl (EFSA PLH Panel, 2019) under field conditions in olive fields in Italy by means of different ways of application for curative purposes. For all the tested products symptoms generally reappeared or proved to be inefficacious to reduce the occurrence and the severity of the desiccation phenomena induced by *X. fastidiosa* on susceptible olive cultivars (Morelli et al., 2021).

A bioactive detergent composed of **plant extracts** from different botanical species, Sulphur, sodium and calcium hydroxide, has been evaluated in olive orchards in Italy, and according to authors, induced recovery (Bruno et al., 2021). Manipulation of the plant mineral levels could be an efficient disease management strategy because in vitro experiments showed that zinc (Zn) detoxification is required for full *X. fastidiosa* virulence, and copper (Cu) influences its growth and biofilm formation (Navarrete and De La Fuente, 2014). In this sense, after application of a Zn- and Cu-containing citric acid biocomplex fertilizer obtained through natural fermentation processes using soil fungi, in infected olive orchards in Italy, by trunk injection or soil drench, re-sprouting of new shoots was observed, but no reduction of disease severity nor pathogen growth was observed in this study (Scortichini et al., 2018; Tatulli et al., 2021). On the contrary, enhanced *X. fastidiosa* virulence was noted in treated plants, with an increase of symptoms and bacterial population levels (Ge et al., 2020). In greenhouse conditions, the application of menadione and benzethonium chloride treatments, abscisic

Funded by the European Union

acid (ABA) and DSF related components, via soil drench, was efficient in reducing PD symptoms in grapevine over a period of three months (Zhang et al., 2019), but did not prevent plants from being re-infected with the pathogen (Meyer and Kirkpatrick, 2011). Direct application to plants surfaces of DSF molecules, palmitoleic acid and macadamia nut oil via spray resulted in a decrease of PD severity (EFSA PLH Panel, 2019). Unfortunately, in all field assays of chemical control to prevent or cure trees from infection, the best situation was that trees seemed to recovery but *X. fastidiosa* was still a resident, and sooner or later disease symptoms re-appeared. Finally, members of this Research Consortium have found that some peptides have antimicrobial and antibiofilm activity against *X. fastidiosa* in vitro (Moll et al., 2021), induce expression of defense genes in almond (Foix et al., 2021), and *Nicotiana benthamiana* (Baró et al., 2022), and reduce bacterial infection. Data related to the use of peptides for the control of *X. fastidiosa* will be detailed within deliverable D6.2 of BeXyl.

For **biological control** of *X. fastidiosa*, some of the strategies that have been explored are endophytes, avirulent or weakly virulent *X. fastidiosa* strains, or phages. In the case of endophytes, *Curtobacterium flaccumfaciens* and *Methylobacterium mesophilicum* have been selected as the most promising bacteria, because certain strains induce systemic acquired resistance (SAR) and show antagonistic activity against *X. fastidiosa*, resulting in a reduction of the *X. fastidiosa* population and a down-regulation of genes involved in growth of *X. fastidiosa* (Dourado et al., 2023). Similar results were obtained with the endophyte *Paraburkholderia phytofirmans*, which was able to easily colonize xylem vessels of grapevines and when inoculated simultaneously or after *X. fastidiosa*, it conferred protection to plants by activation of their induced systemic resistance (ISR) (Baccari et al., 2019; Lindow et al., 2024). Recently, studies of the microbiome in grapevines (Deyett and Rolshausen, 2019) and olive (Vergine et al., 2019; Giampetruzzi et al., 2020) and almond (Anguita-Maeso et al., 2022) have been performed in order to identify more endophytes with potential to be used in biological control, as it has been observed that some resistant cultivars have a more diverse microbiota than susceptible ones. Another approach consists on the use of lytic phages against different *X. fastidiosa* strains in grapevines under greenhouse and field conditions (Das et al., 2015; Stefani et al., 2021) reporting reduction of PD symptoms and lower population levels of *X. fastidiosa*. Recently, in Spain numerous phages that have partial or total lytic activity against several European strains of *X. fastidiosa* have been isolated (Domingo-Calap et al., 2021) and new phages and whose efficacy against *X. fastidiosa* is the object of the present deliverable. The potential use of bacteria as biocontrol agents of *X. fastidiosa* is treated in a different deliverable, specifically in D6.1 entitled 'Development of Synthetic communities (SynComs) of xylem-inhabiting bacteria with key traits against *X. fastidiosa*'.

Funded by the European Union

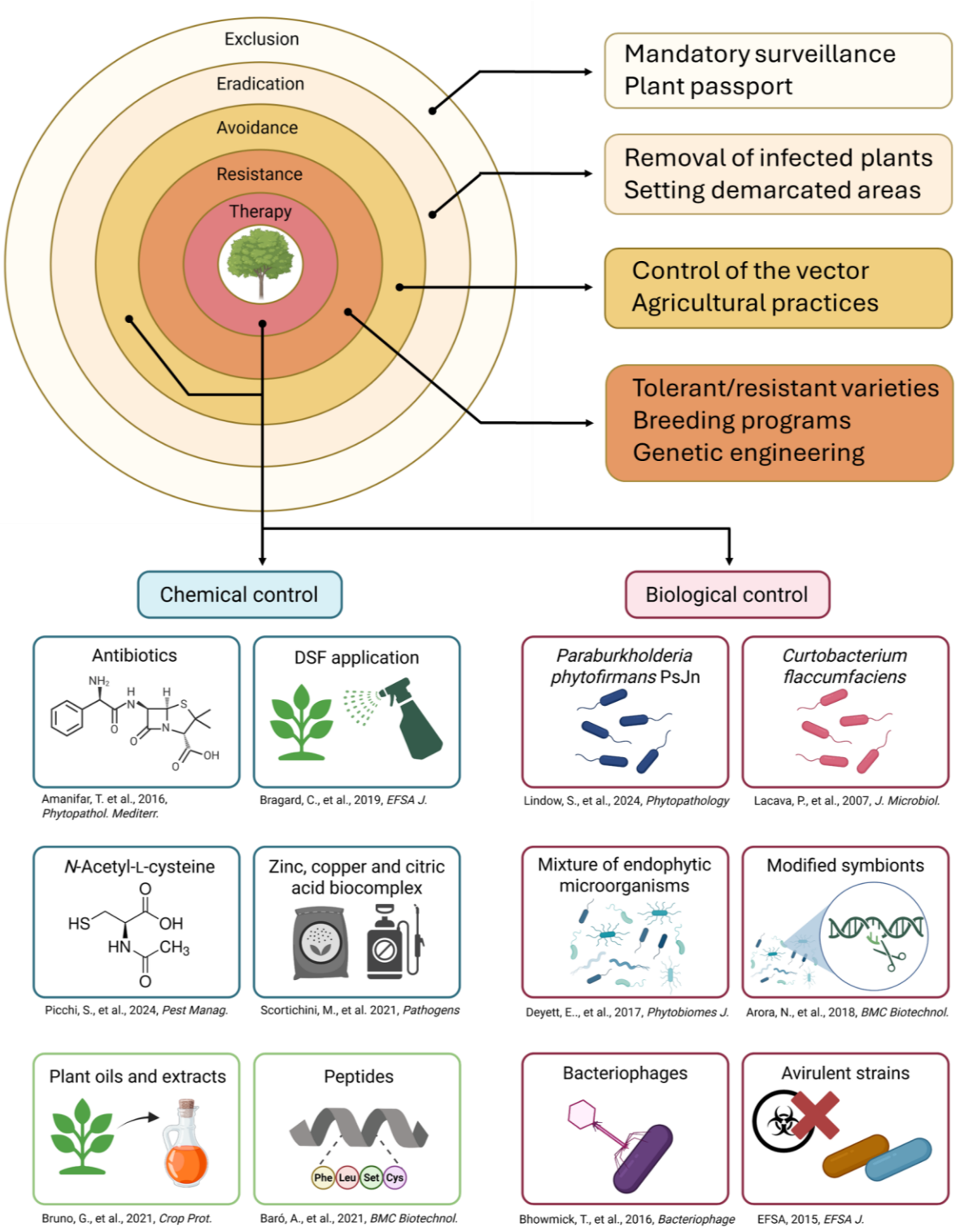


Figure 1: A representation of the different strategies to control *X. fastidiosa* diseases on trees affected by the bacterium fastidiosa (Figure provided by L. Moll from his PhD thesis (Moll, 2024)).

Funded by the European Union

2. METHODOLOGY AND RESULTS

2.1. Vitocristaline glasses and glass-ceramics

2.1.1. Antimicrobial activity of glasses and glass-ceramics

Two glass-ceramic, named as CIN and G3, and one vitrocristraline glass, labelled as G3T were selected for its antimicrobial and biocide activity on planktonic and biofilm formation of cultures of different bacterial and fungal species in previous studies:

G3: G3 is a calcium-rich glass (particle size d< 50 µm). G3T is a vitrocrystalline material obtained from a heat treatment of G3 glass (particle size d< 45 µm). CIN is a ZnO-rich glass (particle size d< 20 µm). G3 is an antimicrobial glass powder, with chemical composition (in mol.%): 40.3 SiO_2, 8.5 B_2O_3, 18.8 Na_2O, 19.2 CaO, 0.57 K_2O, 11.7 Al_2O_3 and 0.12 Fe_2O_3, obtained by the traditional melt-quench process [Moya et al. 2011; Advanced Engineering Materials, 13, B256-B260, doi:10.1002/adem.201080133.]. Briefly, the starting materials were mixed thoroughly and heated in platinum crucibles at 850 ºC for 1 h to allow decarbonation. Subsequently, they were melted at 1400 ºC for 1 h, and then quenched by dipping into water. The glass powder was milled and sieved to < 50 µm, and the corresponding average particle size was found to be d50 = 13 µm.

G3T: The glass-ceramic, labelled as G3T, was obtained after an optimized thermal treatment of glass G3 [Cabal et al. 2014; Scientific Reports 4, doi:10.1038/srep05440.]. Devitrification of G3 glass after thermal treatment at 750ºC lead to a glass-ceramic material composed of combeite ($Na_4Ca_4(Si_6O_{18})$, PDF 75-1687) and nepheline ($Na_{6.65}Al_{6.24}Si_{9.76}O_{32}$, PDF 83-2372) dispersed in a glassy matrix. The glass-ceramic powder was also milled and sieved to < 50 µm (d50 = 10 µm).

CIN: The other glass, CIN, is a ZnO enriched glass, labelled as CIN, that belongs to B_2O_3-SiO_2-Na_2O-ZnO system, with chemical composition (wt.%): 19.29 SiO_2, 34.24 B_2O_3, 5.55 Na_2O, 34.73 ZnO and 5.13 Al_2O_3. This glass was also obtained by melt-quench method (Esteban-Tejeda et al., 2015), fusing a mixture of the required stoichiometric amounts of the different oxides and carbonates of high purity. The glass powder was milled and sieved to < 30 µm (d50= 6.3 µm). These materials were fully characterized by X-Ray diffraction (XRD), Fourier transform infrared spectroscopy (FTIR), Field emission scanning electron microscopy (FESEM) and thermal analysis (Tg-DTA).

Ceramic glasses were prepared as stock solutions at a concentration of 200 mg/mL in aqueous solution and sterilized (autoclave, 121°C, 20min).

Funded by the European Union

In order to assess the bactericidal effect of these antimicrobial compounds several experiments were performed to test their antibacterial activity against different strains of *X. fastidiosa* including two strains from subsp. *fastidiosa* ST1 (IVIA5770, TemeculaL) isolated from grapevine, one of subsp. *multiplex* from ST81 (XYL1752) isolated from a fig tree, and one strain of subsp. *pauca* ST53 (De Donno) isolated from olive tree. All strains were cultured from glycerol stocks on PD3 (Davis, 1981) or BCYE agar (Wells et al., 1981) plates at 28°C in the dark. After 6 to 8 days, cells were re-streaked onto new plates and cultured for 6 days before using them for the experiments.

Xylella fastidiosa colonies were resuspended in PD3 liquid medium and adjusted to a final optical density concentration of 0.08 at 595 nm (OD_{595}) before use. A volume of 2 ml of cell bacterial cultures was transferred to 20-ml borosilicate glass flasks. At time 0, the glass-ceramic materials were added in each flask at final concentration of 5 mg/ml for CIN and 15 mg/ml of G3 and G3T, corresponding to their respective Minimum Inhibitory Concentration (MIC) and Minimum Bactericidal Concentration (MBC) (Cabal et al. 2014, Esteban-Tejeda et al. 2015). A positive control, without glass ceramic, and negative control without bacterial inoculum were included in the study. To ensure an optimal contact between bacterial cells and glass particles, the flasks were incubated were shaken in microbial suspension in a rotary shaker (120 rpm) at 28 °C for 7 days.

At 1, 5, 10, 24 and 48 hours after the addition of the glass-ceramic materials, the number of viable bacteria (colony forming units, CFU/ml) in each suspension was determined by serial dilution plating, and bacterial viability was expressed as log10 CFU/ml. Antimicrobial (bactericidal) efficacy was calculated as the percentage reduction in bacterial counts relative to the untreated control at each time point, using the following formula:

$$\text{Bactericidal Efficacy } (\%) = \frac{\text{Control growth } - \text{ Treatment growth}}{\text{Control growth}}\ x\ 100$$

Additionally, the proportion of live and dead planktonic cells in PD3 broth was estimated for two selected *X. fastidiosa* strains (De Donno and TemeculaL1) using a viability qPCR (v-qPCR) assay (Baró et al., 2020), the TaqMan-based qPCR viability assay developed by Baró et al. (2020) was used to quantify the number of live and dead cells. The percentage of viable cells was estimated using the difference between Cq values of PMAxx treated samples (representing dead cells) and non-treated samples (representing total cells) based on the following formula:

$$\text{Viable cells (\%)} = 100/2^{(\text{Cq PMAxx treated} - \text{Cq non-treated})}$$

The results of colony culturability revealed significant effects of the glass-ceramic treatment ($P<0.05$), exposure time ($P<0.05$), and their interaction ($P<0.05$) on growth of bacterial colony forming units (CFU) on solid medium. These interactions indicate that the antibacterial activity of the nanomaterials was time-dependent (Figure 2). The interaction of *X. fastidiosa*

Funded by the European Union

cells with the glass-ceramic materials demonstrated a progressive inhibition of bacterial growth, with complete suppression of viable colonies and a 100% of antibacterial efficacy (%) observed in G3 and G3T treatments after 48 hours of exposure (Figures 3 and 4, respectively).

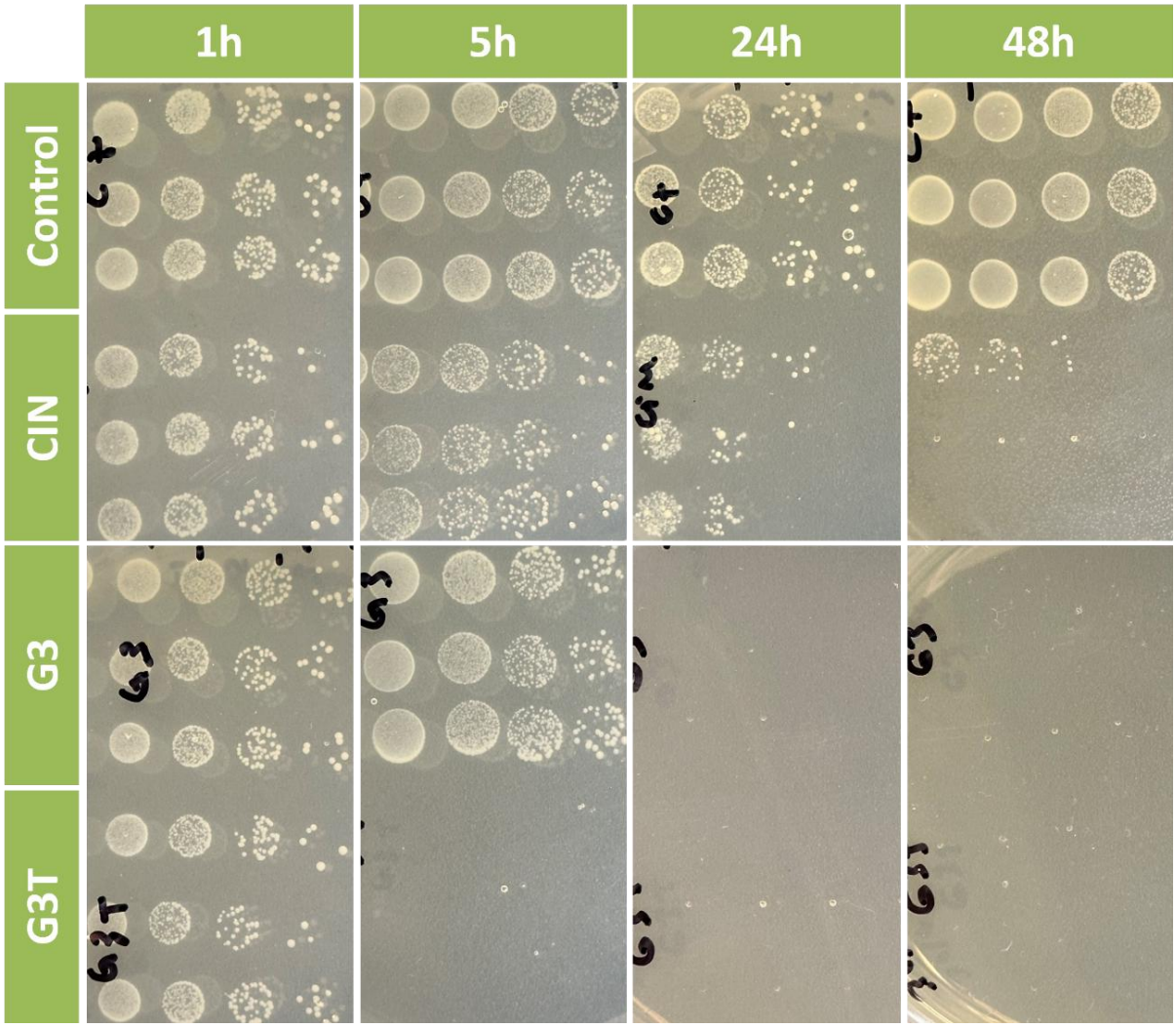


Figure 2: Bacterial growth after treatment with the glass ceramics CIN and G3 and the vitrocristraline glass G3T compared with Control for *Xylella fastidiosa* subsp. *fastidiosa* strain IVIA5770. Images were captured at 1, 24, and 48 hours after inoculation, showing the progression of bacterial inhibition over time under different treatment conditions. In each picture the spots from left to right correspond to colonies developed from 1/10 serial dilutions of bacterial cultures.

Funded by the European Union

The log(CFU/mL) values obtained for all glass-ceramic treatments compared to untreated control are shown in Figure 2. All strains exhibited significantly lower bacterial log(CFU/ml) values after glass-ceramics treatments ($P < 0.05$), although the extent of reduction depended on the exposure time. The mean log(CFU/ml) of untreated control cultures ranged from 6.23±0.11 to 8.8±0.22. No significant differences were observed for growth in the controls ($P \geq 0.05$) over 48 h of incubation (Figure 2).

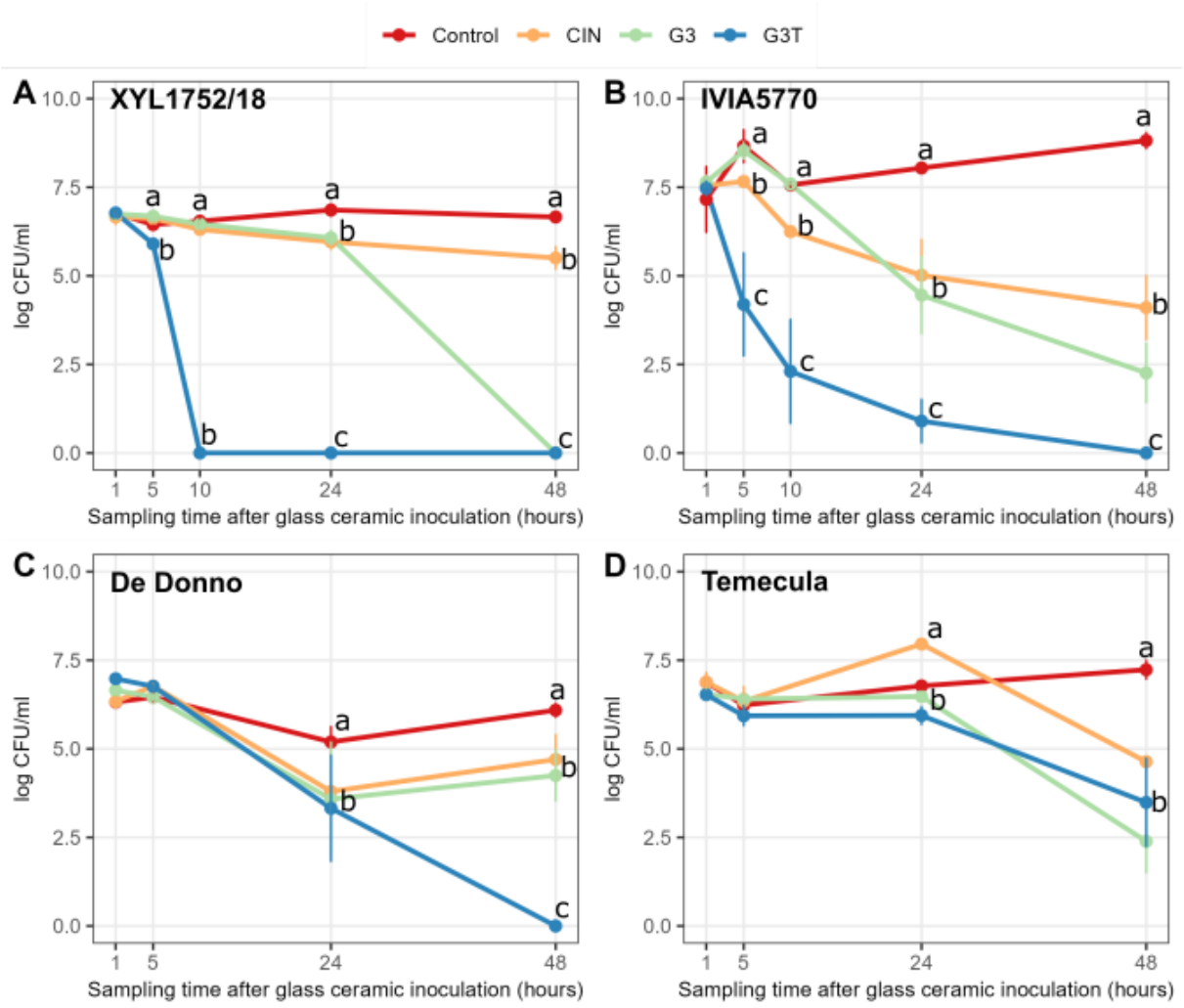


Figure 3: Bacterial colonies (log CFU/ml) of four *Xylella fastidiosa* strains, XYL1752/18 (A), IVIA5770 (B), De Donno (C), and TemeculaL (D) developed after treatments with glass ceramics CIN and G3 and the vitrocristraline glass G3T evaluated at different sampling times (1, 5, 10, 24, and 48 hours) of exposure. Vertical lines represent the standard error of the mean. Bars with different letters indicate significant differences ($P < 0.05$) at the same sampling time.

In general, exposure times of cell suspensions with glass-ceramics shorter or equal to 5 hours did not significantly affect bacterial growth ($P \geq 0.05$), except for the strain XYL1752/18 showing a significant and slight growth inhibition compared to control reaching 5.9±0.07 a log(CFU/ml) after 5 h. After 10 hours, treatment with G3T in strains IVIA5770 and XYL1752/18

Funded by the European Union

showed a significantly (P<0.05) log(CFU/ml) reduction, achieving 2.3±1.46 log(CFU/ml) and a complete suppression of viable colonies, respectively (Figure 3).

After 24 hours of incubation, the G3T treatment exhibited the highest bactericidal effect as compared to CIN and G3, although responses varied among strains. Complete growth inhibition of the strain XYL1752/18 was maintained with G3T treatment, followed by CIN and G3, showing a lower (P<0.05) cell culturability (<6.1 log(CFU/ml)) compared to control. For IVIA5770 strain, G3T was the most effective treatment, reaching 0.9±0.61 log(CFU/ml) and was significantly (P<0.05) most effective than the treatment with CIN (5.0±1.00 log(CFU/ml)) and G3 (4.5±1.08 log(CFU/ml)). De Donno strain showed a significant reduction of <3.8 log(CFU/ml) compared to control (P<0.05), with no significant differences among glass-ceramic treatments. In contrast, TemeculaL did not show a significant difference in log(CFU/ml) values among treatments after 24 h (Figure 3).

The highest bactericidal activity across all treatments was observed after 48 hours of exposure. G3T was the most effective glass-ceramic, resulting in a complete growth inhibition for all strains except for TemeculaL which showed log(CFU/ml) values ranging from 2.4±0.88 to 4.6±0.15. G3 treatment showed also a significant reduction of viability for all strains with reductions ranging from log(CFU/ml) 4.5±0.69 for De Donno strain to a complete growth inhibition (P <0.05). CIN had the lowest inhibitory effect, though it still resulted in significant (P < 0.05) reductions in log(CFU/ml) values compared to the control (i.e., log(CFU/ml) <5.5) (Figure 3).

The estimated antibacterial efficacy of the glass-ceramics against *X. fastidiosa* revealed significant effects of glass-ceramic treatment (P<0.001), exposure time (P<0.001), and their interaction (P<0.001). The antibacterial efficacy of the glass-ceramics against *X. fastidiosa* was time-dependent.

During early exposure periods (from 1 to 10 hours), minimal antibacterial activity was observed for all treatments, with the exception of the GT3 treatment for strains XYL1752/18 and IVIA5770. After 10 hours of treatment, GT3 achieved 100% efficacy for XYL1752/18 and 69.1% for IVIA5770 (P<0.05), whereas CIN and G3 exhibited limited activity, with antibacterial efficacy values remaining below 17.4% for all strains.

After 24-hour of exposure, G3T continued showing the highest antibacterial efficacy, with significant differences (P<0.05) compared to CIN and G3. G3T achieved 100% efficacy for XYL1752/18, 88.2% for IVIA5770 and 12.0% efficacy for TemeculaL. For De Donno strain, the antibacterial efficacy of G3T reached 50%, with no significantly differences among treatments. After 24 hours, G3 and CIN showed a lower antibacterial efficacy compared to G3T for XYL1752/18 (<8.8%) IVIA5770 (<42.1%) and TemeculaL (<4.7%).

Funded by the European Union

Maximum antibacterial efficacy was reached after 48 hours of exposure for all strains and treatments. At this time point, G3T achieved complete bacterial growth suppression for XYL1752/18, IVIA5770, and De Donno, and 64.1% efficacy against TemeculaL. GT3 showed significant differences (P<0.05) with CIN and G3 treatment for all strains, except for the strain XYL1752/52 treated with G3, reaching moderate efficacy levels ranging from 13% to 75.9%.

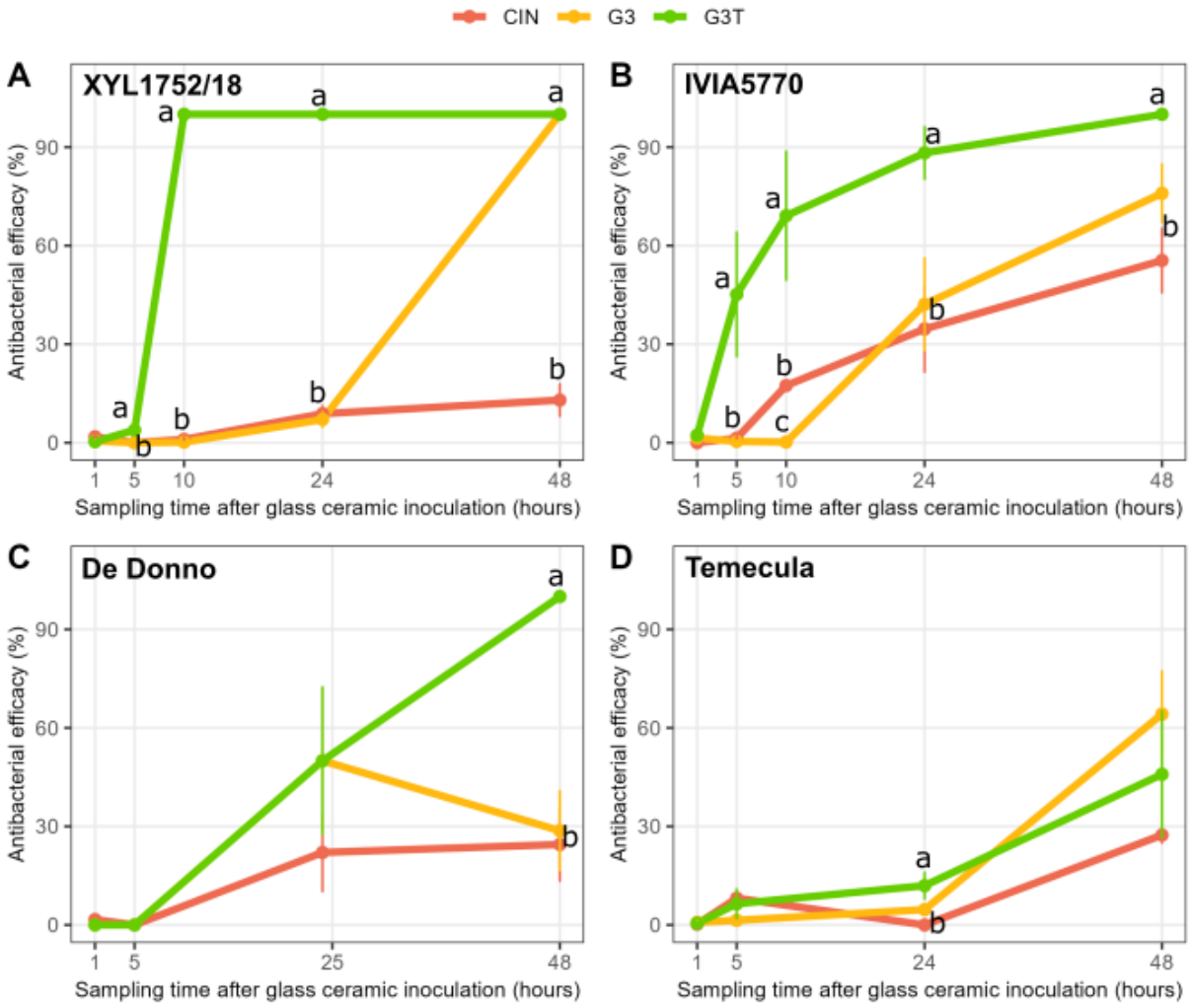


Figure 4: Antibacterial efficacy (%) after treatment with glass ceramics CIN and G3 and the vitrocristraline glass G3T against four *Xylella fastidiosa* bacterial strains, XYL1752 (A), IVIA5770 (B), De Donno (C), and TemeculaL (D), evaluated at 1, 5, 10, 24, and 48 hours after glass-ceramics exposure. Vertical lines represent the standard error of the mean. Bars with different letters indicate significant differences (P < 0.05) at the same sampling time.

The percentage of viable *X. fastidiosa* cells, estimated through v-qPCR assay, demonstrated significant time-dependent cytotoxic effects in response to glass ceramic treatments (Figure 4). For both strains tested, De Donno and TemeculaL, treatment (F=3.9, P=0.021) and exposure time (F=8.7, P=0.007) had a significant influence on cell viability, while the interaction between these two factors was not statistically significant.

Funded by the European Union

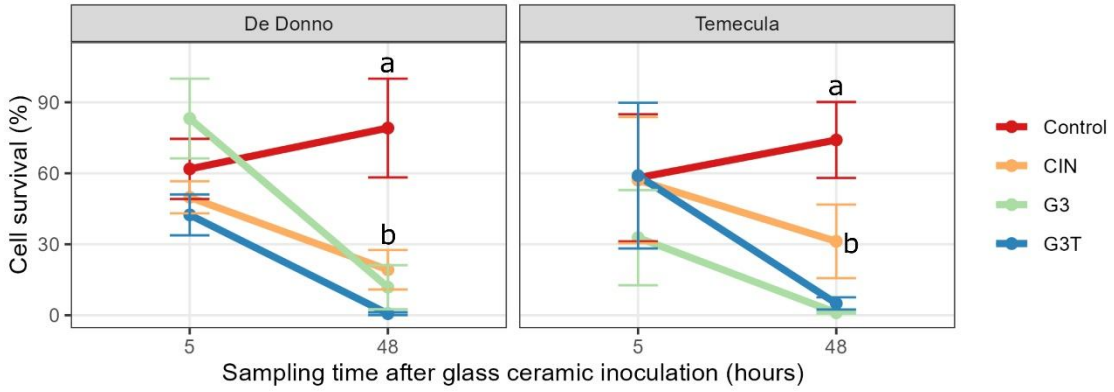


Figure 5: Percentage of cell viability for *Xylella fastidiosa* strains De Donno and TemeculaL after treatment with glass ceramics CIN, G3, and G3T after 6 and 48 hours of exposure measured by a viability qPCR assay (Baró et al. 2020). Each point represents the mean cell survival (%) of at least three biological replicates under the same conditions. Vertical lines represent the standard error of the mean. Bars with different letters indicate significant differences ($P < 0.05$) at the same sampling time.

At 5 hours post-treatment, bacterial survival rates varied depending on the glass ceramic treatment; however, no significant differences ($P>0.05$) were observed among them, obtaining bacterial cell survival from 42.4 to 83.2 % for De Donno and from 32.8 to 59.0 % for TemeculaL (Figure 5).

After 48 hours of glass ceramics treatment, a significant ($P<0.05$) reduction in viability was observed. For both strains, cell viability of control treatment was significantly ($P<0.05$) higher (>79.1%) compared to glass ceramic treatments (<31.2%). Although there were no significant differences among glass-ceramic formulations, G3T consistently exhibited the strongest cytotoxic activity, reducing viable cells to values between 0.7% and 5.0% for De Donno and TemeculaL, respectively. G3 treatment resulted in 1.07% to 11.8% cell survival, while CIN showed a more moderate effect, with viability ranging from 19.2% to 31.3% for De Donno and TemeculaL strains, respectively (Figure 5).

2.1.2. Phytotoxic activity of glasses and glass-ceramics

Glasses and glass ceramics were evaluated for their phytotoxic effect after infiltration into tobacco (*Nicotiana benthamiana*). Tobacco plants were grown from seed in a greenhouse under controlled conditions and used with 30-40 days old. Plants were cultivated in pots containing a sterile mixture of acidic peat, neutral peat, wetting agent, and a supplemented compound mineral fertilizer (NPK) (Flora gard, Oldenburg, Germany).

Glass ceramics suspensions (100 µl) were applied at concentrations ranging from 1 to 15 mg/ml for CIN and from 2.5 to 25 mg/ml for G3 and G3T. Suspensions of each treatment were infiltrated into the mesophyll of fully expanded leaves using a needleless syringe. Three independent repetitions were performed in three plants, for each treatment and concentrations were randomly distributed in the plant leaves; the experiment was repeated

Funded by the European Union

twice. Water, PD3 and bleach were used as negative and positive controls, respectively. Plants were maintained under greenhouse conditions (25 ± 2 °C).

Seven days post-infiltration phytotoxicity was assessed based on a binary response (presence or absence of leaf damage) and by measuring the diameter of necrotic lesion. The effective concentration (EC_{50}) causing visible damage in 50% of infiltrated leaves was determined for each treatment and defined as the minimum concentration resulting in necrosis in ≥50% of the evaluated leaves.

Overall, all tested compounds exhibited some degree of phytotoxicity on tobacco leaves, varying according to the concentration. Leaf damage consisted mainly on necrotic spots, with some leaves showing chlorotic halos (Figure 6).

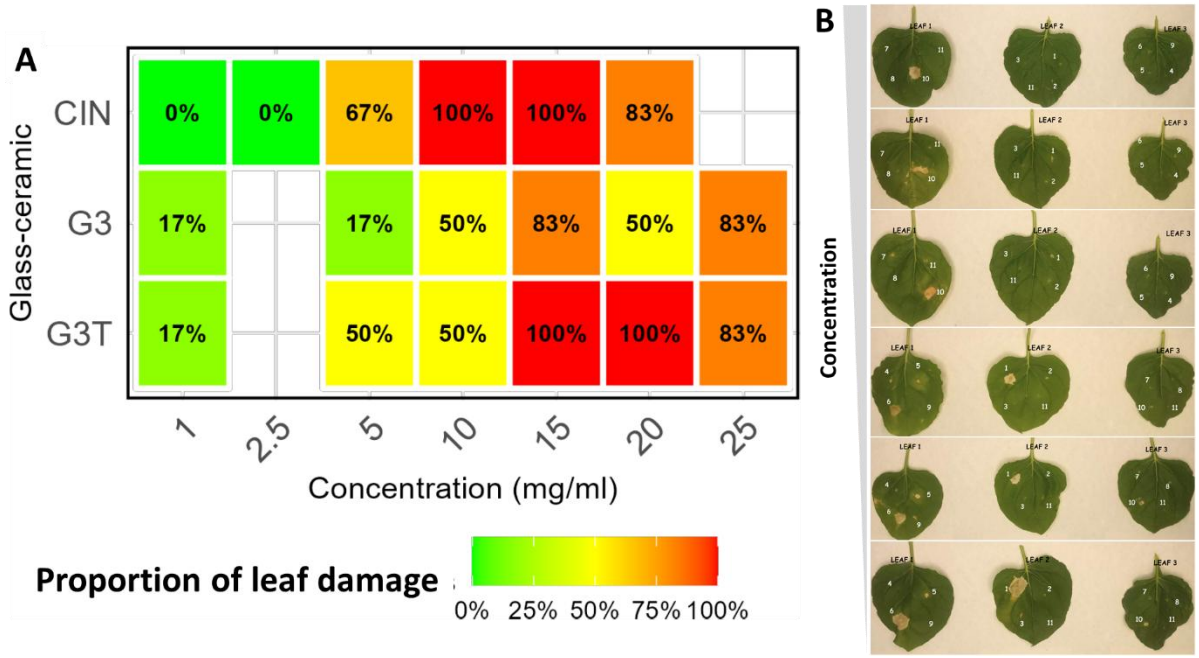


Figure 6: Phytotoxicity on leaves on *Nicotiana benthamiana* caused by different glass-ceramics infiltrated at various concentrations. (A) Heatmap showing the proportion of leaf damage. (B) Tobacco leaves exhibiting varying degrees of necrosis seven days post-infiltration with the tested compounds. Treatments: 6=CIN; 7=G3; 8=G3T; 9=water; 10= bleach; 11= PD3.

Funded by the European Union

2.2. Plant extracts

2.2.1. Antimicrobial activity of extracts from 'alperujo'

A total of five antimicrobial plant extracts enriched in different compounds were obtained from 'alperujo' (the main by-product of olive oil processing) or from their anaerobic digestion of the remaining solid waste after thermal pre-treatment (Figure 7):

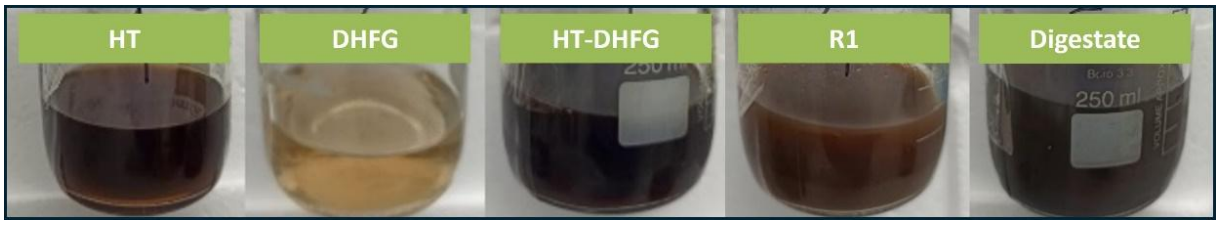


Figure 7: Alperujo liquid extracts tested against *Xylella fastidiosa* strains.

Hydroxytyrosol (HT): An extract with a concentration of 20 g/L of (HT) in water, which is one of the most active phenolics present in olives both in free form and forming conjugates, was obtained from liquid effluents of the olive oil industry by physical procedures through chromatographic adsorption and subsequent concentration of the sample. This process is patented (Patent WO 2013/007850A1).

4-Dihydroxyphenylglycol (DHFG): An extract with a concentration of 220 ppm DHFG in water obtained from olive leaves obtained by using a physical patented procedure (P202030495) by means of a specific heat treatment and chromatographic purification. This is a phenolic, like hydroxytyrosol, but with one more OH group in the aliphatic chain. It has phyto-regulatory activity by mimicking an allelopathic substance and its use as a phyto-regulator has been patented for the formulation of natural herbicides (Patent P201631404).

3,4-dihydroxyphenylglycol + hydroxytyrosol + oleuropein (HT-DHFG): This is a mixture of the two most active phenols in olives in a more favourable ratio of DHFG, with HT and oleuropein derivatives at a concentration in water of 216 ppm DHFG + 134,5 ppm HT and a similar proportion of elenolic acid derivatives. Oleuropein is the most abundant phenol in olives and is one of the main precursors of HT. The extract has been obtained from olive leaf in the same procedure for obtaining and purifying DHFG (P202030495) in one of the fractions downstream of DHFG.

Phenol-rich digest of 3,4-dihydroxyphenylglycol and hydroxytyrosol (R1): An extract containing 125 ppm DHFG + 50 ppm HT obtained from a liquid effluent obtained from a heat treatment of 'alperujo' by heat treatment at 180°C for one hour followed by centrifugation to separate the phases, and finally an anaerobic digestion on the liquid phase under special pH conditions to favor the accumulation of phenolics rather than their degradation.

Digestate O-Phenols (Digestate): This is an extract in which the phenols have been completely degraded but contains the degradation products of the organic matter plus those

Funded by the European Union

of the phenols. It has been extracted from a liquid effluent obtained from the heat treatment of 'alperujo' at 180 ºC for one hour, followed by centrifugation to separate the phases, and a final anaerobic digestion applied to the liquid phase, promoting the methanisation phase instead of remaining in the acidification phase, promoting the degradation of the phenolic compounds.

All plant extracts derived from "alperujo" were prepared following the next protocol. Firstly, 50% extract stock was prepared by mixing equal volumes of pure extract and PD3 liquid medium. The 50 % concentration was subsequently diluted to obtain five concentrations 25%, 12.5%, 6.25%, 4%, and 2% (v/v) of the original extract by mixing appropriate volumes from 50% extract with sterile distilled water, ensuring that the final concentration of PD3 remained constant across all treatments.

The antibacterial activity of the five "alperujo" extracts was tested against six *X. fastidiosa* strains from subspecies *fastidiosa* (TemeculaL and IVIA5770 of ST1 isolated from grapevines and IVIA5235 of ST1 isolate from a cherry tree), *multiplex* (IVIA5901 and Dixon of ST6 and TOS4 of ST87 isolated from almond trees) and *pauca* (De Donno of ST53 isolated from an olive tree). All strains were cultured from glycerol stocks on PD3 (Davis, 1981) or BCYE agar (Wells et al., 1981) plates at 28°C in the dark. After 6 to 8 days, cells were re-streaked onto new plates and cultured for 6 days before using them for the experiments.

The antibacterial activity of the 'alperujo' extracts was evaluated in PD3 liquid medium using polystyrene 96-well microtiter plates inoculated with 220 µl of each 'alperujo extract inoculated with a bacterial suspension (OD_{600} = 0.08) of each *X. fastidiosa* strain, with five replicated wells per treatment and strain. An equal number of wells were filled with PD3 and all the plant extracts concentrations as negative control. Microplates were incubated at 28 for 7 days in the dark without agitation. The optical density at 595 nm (OD_{595}) was measured daily using an i-Mark TM microplate absorbance reader spectrophotometer (Bio-Rad, Hercules, CA, USA). At the end of the experiment the biofilm formation was estimated using the crystal violet assay (Zaini et al., 2009) by measuring OD_{595} as described in detail in section 2.3.1.

Growth curves were obtained from the accumulated OD_{595} over time up to 7 days, and the standardized area under the OD_{595} progress curve (SAUGPC) was calculated using the trapezoidal integration method, standardized by the duration of the experiment in days (Simko & Piepho, 2011). Additionally, at 1, 6, 24 and 48 hours after *X. fastidiosa* inoculation, the cell culturability of *X. fastidiosa* cells for each strain after the treatment with the 'alperujo' extracts was assessed by inoculating 8 µl from planktonic cells of each well onto PD3 agar plates. Cell viability was determined after 15 days by observing colony development on the culture media. The results were recorded as binary values of "0" for no growth and "1" for growth". The Minimum Inhibitory Concentration (MIC) was defined as the lowest concentration at which no growth occurred in at least 50% of replicates. Treatment combinations with no inhibitory effect, (NE), indicated that the maximum concentration tested was insufficient to achieve some inhibitory threshold.

Funded by the European Union

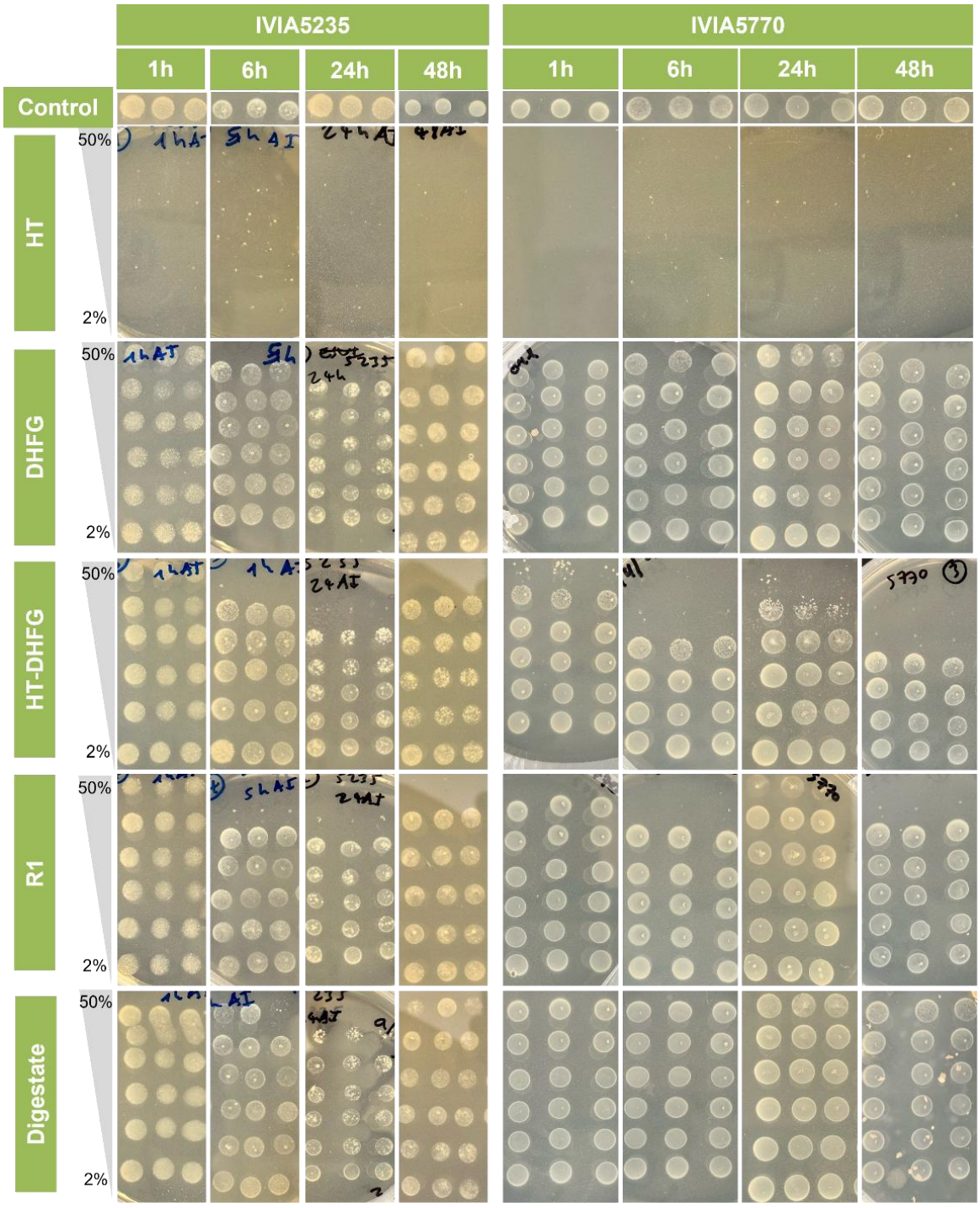


Figure 8: Bacterial growth developed on PD3 solid medium after treatment with five extracts obtained from "alperujo" (HT, DHFG, HT-DHFG, R1 and Digestate) tested against *X. fastidiosa* strains IVIA5770 and IVIA5235 at four at four exposure times (1, 6, 24, and 48 hours) after treatment.

Figure 8 shows the antimicrobial activity of the five "alperujo" derived extracts tested at different concentration (from 2 to 50%) on colony growth of two *X. fastidiosa* strains (IVIA5235 and IVIA5770) over time. The results reveal varying distinct levels of bacterial growth inhibition among the treatments compared with control. Among them, the HT extract

Funded by the European Union

exhibited the highest bactericidal activity even at the lowest concentrations tested. DHFG and R1 treatments showed inhibitory effects only at the highest concentrations (>25%). In contrast the DHFG and Digestate extracts did not had effect on subsequent colony growth development.

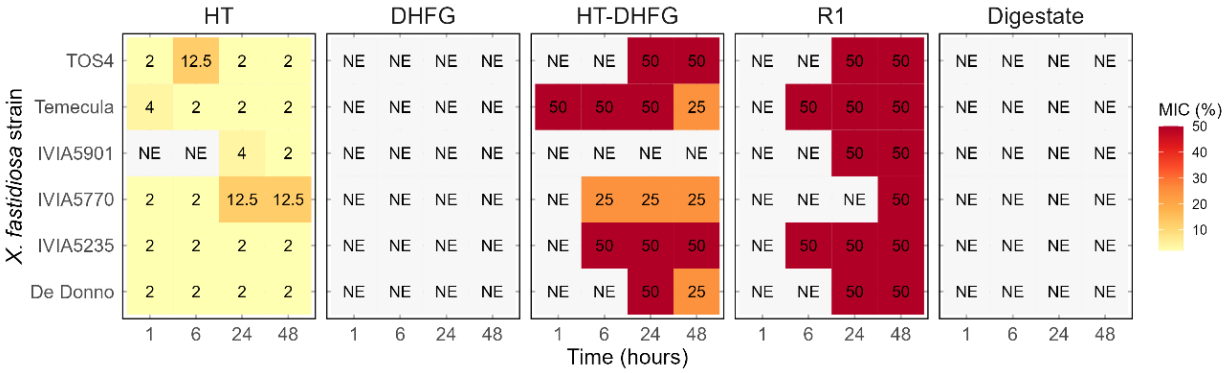


Figure 9: Minimum Inhibitory Concentration (MIC) for six *Xylella fastidiosa* strains (TOS4, Temecula, IVIA5901, IVIA5770, IVIA5235, and De Donno) after treatment with five extracts from "alperujo" (HT, DHFG, HT-DHFG, R1 and Digestate) at four exposure times (1, 6, 24, and 48 hours) after treatment.

The minimum inhibitory concentration (MIC) of five plants extracts from alperujo against six *X. fastidiosa* strains is shown as a heatmap in Figure 9. All hydroxytyrosol-containing extracts and extract R1 had some inhibitory activity against *X. fastidiosa*. The plant extract with the highest growth inhibition at the lowest concentrations was HT, which exhibited consistent inhibitory activity against all *X. fastidiosa* strains tested at low concentrations (2-4%), with the exception of the IVIA5770 strain which required higher concentrations (12.5%) of HT, and for extended exposure times. The HT-DHFG extract also exerted some inhibitory activity, with a variable response among strains. Most of the strains tested showed no growth after HT-DHFG treatment at 50% concentration for 24 hours, with the exception of strain IVIA5901. Strain IVIA5770 was also inhibited at a concentration of 25% HT-DHFG. The R1 extract showed inhibitory activity patterns comparable to those observed for HT-DHFG, requiring exposure times of at least 24 hours at a 50% concentration to be effective against most *X. fastidiosa* strains tested. In contrast, treatments with DHFG and digestate did not result in detectable inhibitory effects against any of the tested strains at any of the concentrations and exposure times evaluated (Figure 9).

Funded by the European Union

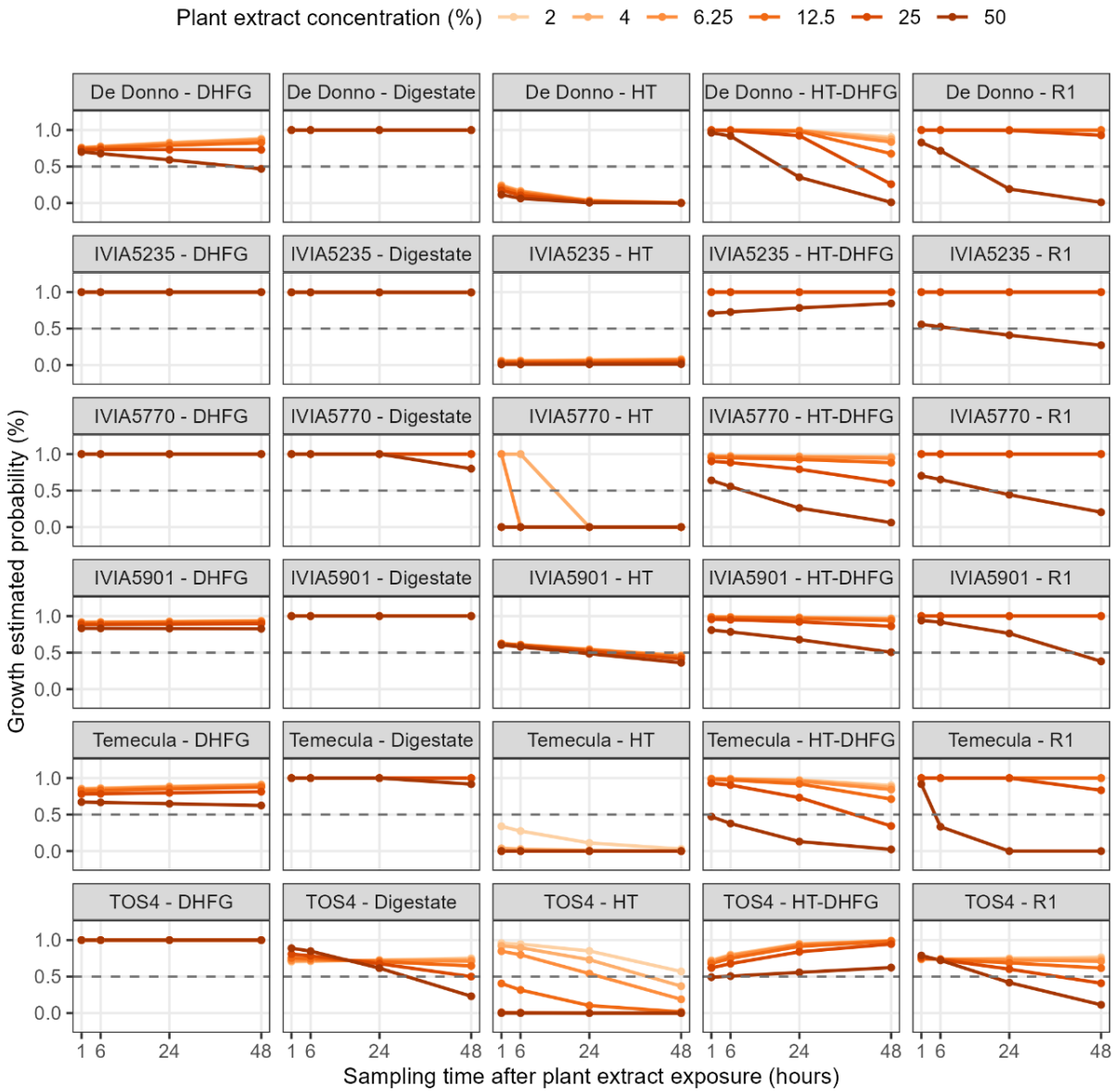


Figure 10: Growth estimated probability (%) for the six *Xylella fastidiosa* strains (TOS4, Temecula, IVIA5901, IVIA5770, IVIA5235, and De Donno) after treatment with five extracts from "alperujo" (HT, DHFG, HT-DHFG, R1 and Digestate) at four exposure times (1, 6, 24, and 48 hours) after treatment.

Binary logistic regression models were fitted separately to the six *X. fastidiosa* strains to estimate the probability of bacterial growth in response to five treatments, six concentrations, and 4 incubation times (1, 6, 24, and 48 h) (Figure 10). All models revealed quasi-complete separation, indicating a high level of predictability in response variables. Model performance was consistently strong, obtaining AUCROC curves above 0.86 for all strains, and robust associations between predicted and observed outcomes were oberved. For all the strains, treatment had a significant effect on bacterial growth probability (χ^2>16.5, *P*<0.001), as well as strong and highly significant interactions between treatment ×

Funded by the European Union

concentration (χ^2=427.81, *P*<0.001), and treatment × time (χ^2=443.88, *P*<0.001), except for the strains IVIA5235 and IVIA5770. Distinct response profiles were observed among the six *X. fastidiosa* strains across treatment, concentration, and incubation time (Figure 10). Nevertheless, all models consistently estimated a low probability of bacterial growth treated with HT, which exhibited the strongest bactericidal effect across all strains and was effective at the lowest concentrations tested compared to other treatments. For HT-DHFG and R1 alperujo extracts, growth suppression was more evident at later incubation times (>24 hours) and at moderate-to-high concentrations (>25%). These treatments produced a moderate bactericidal effect, reflected by a decline in predicted growth probabilities, particularly for strains De Donno, IVIA5770 and Temecula (Figure 10).

The quantification of biofilm formation using crystal violet staining at 7 days post-treatment revealed that nearly all tested treatments reduced biofilm development compared with untreated control across all tested strains. Although most treatments, except HT at all concentrations and DHFG-HT and R1 and concentration higher than 25%, allowed colony growth after planktonic cell plating up to 48 post treatment, significant reductions in biofilm formation were obtained after 7 days of incubation in almost all treatments (data not shown). Despite variability in biofilm inhibition efficacy among the tested strains, a general trend of dose-dependent biofilm inhibition was observed. The plant extracts R1, Digestate and DHFG-HT demonstrated the highest levels biofilm inhibition, achieving mean reductions between 80.7 and 85.2% compared to controls. These were followed by HT (64.7%) and DHFG (55.68%) extracts. In general, higher concentrations of alperujo extracts were associated with greater biofilm inhibition, with the maximum effect observed at the 50% concentration (80.6%). Lower concentrations also produced significant inhibitory effects, with mean biofilm reductions ranging from 67.6 to 74.7%.

Additionally, extracts from 'alperujo' were evaluated for their phytotoxic effect after infiltration into tobacco (*Nicotiana benthamiana*) as described in section 2.1.2. Plant extracts were tested at concentrations ranging from 2% to 50%. HT and HT-DHFG demonstrated the highest toxicity, causing foliar damage in 100% of infiltrated leaves even at the lowest tested concentration with an effective concentration of 2% (Figure 11). DHFG extract showed moderate toxicity, inducing 67-83% leaf damage at low concentrations with EC_{50} = 4%. Conversely, the R1 and digestate plant extracts showed the lowest phytotoxic activity (EC_{50} = 12.5% and 4%, respectively). These extracts caused minimal phytotoxicity (0 to 50%) at concentrations below 6.25%, although leaf damage increased to 67% and 83% at the highest tested concentration (50% for digestate and 12.5-25% for R1). Notably, HT, that was identified as the most effective plant extract against *X. fastidiosa* in vitro, was also the most phytotoxic to tobacco plants (Figure 11).

Funded by
the European Union

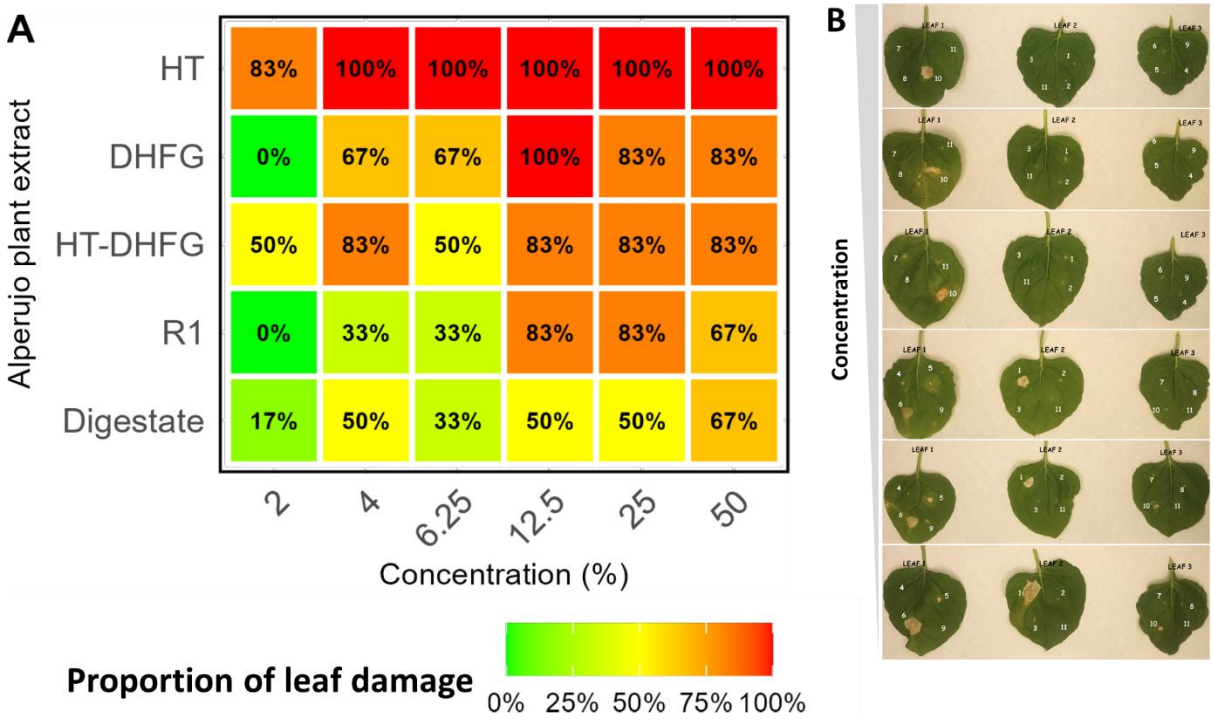


Figure 11: Phytotoxicity on leaves on *Nicotiana benthamiana* caused by different alperujo extracts infiltrated at various concentrations. (A) Heatmap showing the proportion of leaf damage. (B) Tobacco leaves exhibiting varying degrees of necrosis seven days post-infiltration with the tested compounds. Treatments: 1=HT; 2=DHFG; 3=HT-DHFG; 4=R1; 5=Digestate; 9=water; 10= bleach; 11= PD3.

2.2.2. Eucalyptus essential oil

Results from this section have been published in a manuscript (Montesinos et al. 2023, https://doi.org/10.3389/fpls.2023.1122218). Consequently, only main findings are reported here.

The activity of an eucalyptus essential oil (main components 1,8-cineole (>70), limonene (<10%) and α-Terpineol (<10%)) against *X. fastidiosa* was studied using growth inhibition and contact assays, and the pathogen was susceptible to the formulation EGL2. The bactericidal effect was strong causing 4.5 to 6.0 log reductions in survival in 30 min at concentrations in the range of 0.75 to 15.0 ml/ml. Transmission electron microscopy (TEM) of the formulation EGL2 against the three *X. fastidiosa* subspecies studied allowed the observation of a strong lytic effect on bacterial cells (Figure 12).

Funded by the European Union

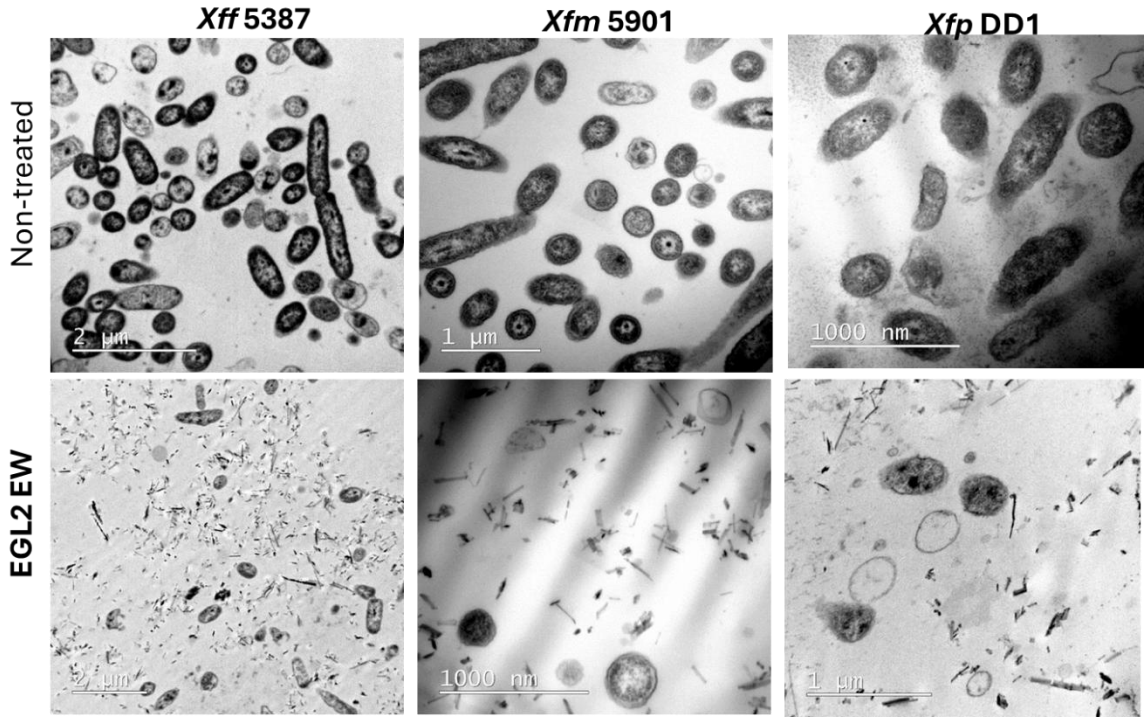


Figure 12: Transmission electron microscopy microscopy of samples of *Xylella fastidiosa* subsp. *fastidiosa* IVIA 5387.2, subsp. *multiplex* IVIA 5901.2 and subsp. *pauca* De Donno after exposure to EGL2 at 6 µl/ml for 120 *min.* Notice that very few cells remain intact after the treatment, and extensive lysis and debris material is observed (lower panels).

Almond plants treated by endotherapy or soil drenching, and then inoculated with *X. fastidiosa* showed a significant decrease in disease severity of almond leaf scorch (ALS) and a delay on symptoms onset as well as a reduction in the levels of the pathogen as measured by qPCR, depending on the strategy used (endotherapy/soil drenching, preventive/curative) (Figure 13). No phytotoxic effects were observed on the treated almond plants.

The treatment by endotherapy in almond plants induced the expression of several genes involved in plant defense after 24 h of treatment. Specifically, transcript levels increased for the genes 7S globulin-like, glutamate receptor, G-type lectin S-receptor-like serine/threonine-protein kinase, pathogenesis-related transcriptional activator PTI5, PR9, RING-H2 finger and pathogenesis-related protein 4, in comparison to non-treated control plants. It was concluded that the reduction of infections by the eucalyptus oil treatments was due to the combination of its bactericidal and plant defense induction activities.

Funded by
the European Union

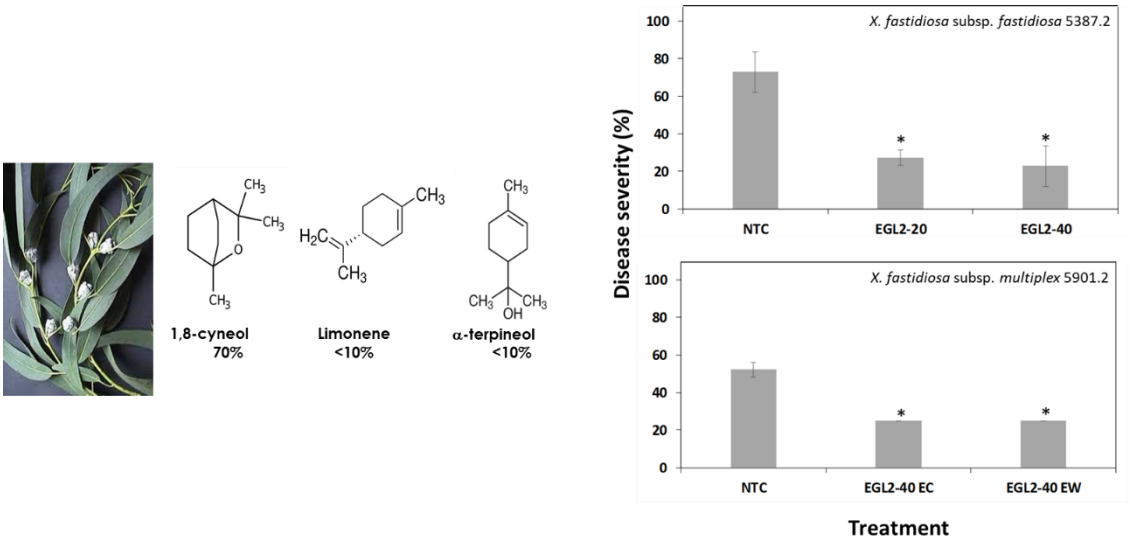


Figure 13: Disease severity of almond leaf scorch in almond plants treated with EGL2 by endotherapy and infected by *Xylella fastidiosa* subsp. *fastidiosa* IVIA 5387.2 or *X. fastidiosa* subsp*. multiplex* IVIA 5901.2. Values are the means of three replicates of three plants, and error bars represent the standard deviation of the mean. Different letters between treatments indicate significant differences in disease severity according to Tukey's test ($P \leq 0.05$).

2.3. Peptides

2.3.1. Activity of single peptides

Most of the results obtained in this deliverable 6.2 concerning the activity of single peptides for the control of *X. fastidiosa* have been already published (Baro et al., 2022, doi:10.3389/fpls.2022.1061463; Moll et al., 2022, doi: 10.1094/PHYTO-12-21-0525-R; Montesinos 2023, https://doi.org/10.1146/annurev-phyto-021722-034312; Moll et al., 2024, https://doi.org/10.1007/s00299-024-03276-x; Moll et al., 2025, https://doi.org/10.1094/PDIS-07-24-1414-RE). Consequently, only main results will be described in the present deliverable.

Several single peptides were synthetized using solid-phase methods, at mg levels for the in vitro studies and at g level for in planta experiments. The compounds were obtained as acetate salts and were analyzed to verify that they have the expected sequences and their degree of purity. In all cases the purity was higher than 95%.

Funded by the European Union

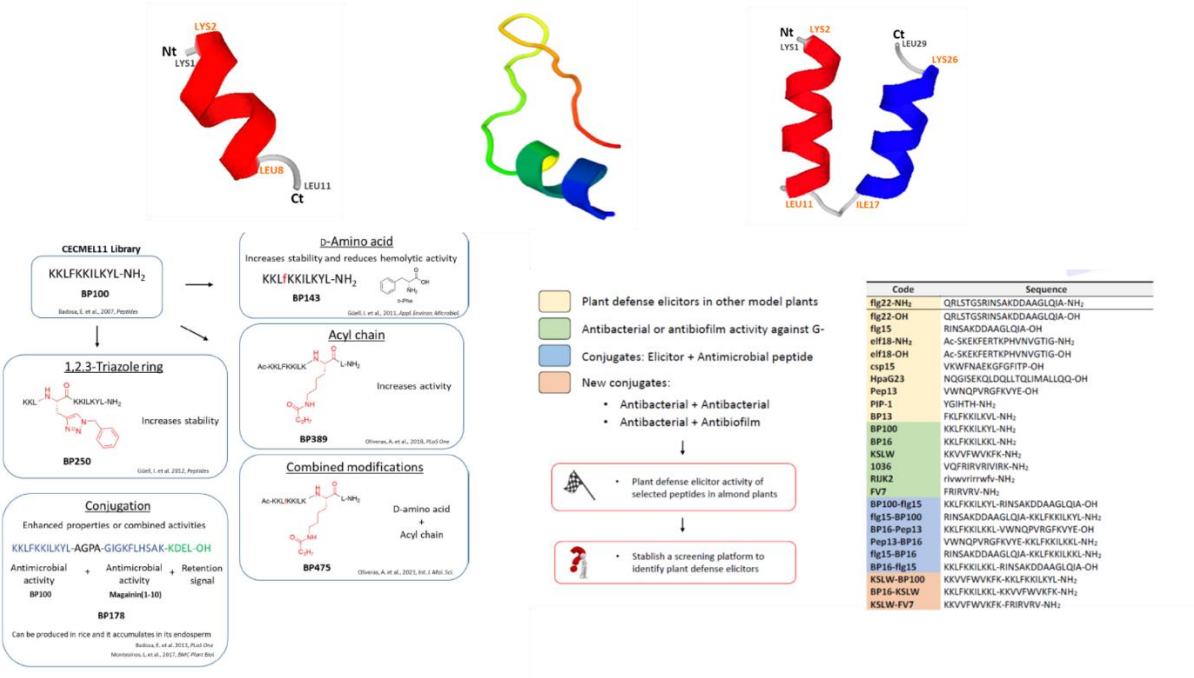


Figure 14: Structures and sequences of some of the representative peptides synthetized and evaluated for the control of *Xylella fastidiosa.*

The effect of seven selected peptides (BP178, FV7, HH15, 1036, BP473, Pep1 and Pep2; Figure 14) on culturability, bactericidal activity, and antibiofilm activity was assessed against five *X. fastidiosa* STs (ST1 and ST2 of subsp. *fastidiosa*; ST6 and ST7 of subsp. *multiplex*, and ST53 of subsp. *pauca*). The effect on culturability and bactericidal activity was tested by a contact exposure test. Peptides were tested at a final concentration of 50, 12.5 and 3.1 µM. Briefly, 20 µL of the corresponding peptide dilution were mixed with 180 µL of a *X. fastidiosa* suspension at 10^7 CFU/mL in tubes. The tubes were incubated at 25 °C and the peptide's activity was determined at 30 min or 3 h. Three replicates for each concentration, peptide, strain, and sampling time were performed.

To assess the effect on culturability, plate counting was performed by plating 20 µL of 10-fold dilutions on PD2 agar plate, and colony forming units were determined after incubating them at 28 °C for 7-17 days. The bactericidal activity was also determined for the peptides that showed activity identified in the culturability test (>2.5 logs of population reduction) by using a qPCR viability assay (Baró et al., 2020; Figure 15). Briefly, samples were treated with PMAxx (VWR, Spain) to a final concentration of 7.5 µM, and they were incubated for 8 min in the dark at room temperature following a photoactivation of 15 min. DNA extractions of all samples were performed using the GeneJET Genomic DNA purification Kit (Thermo Fisher Scientific, United States of America) following the specific protocol for Gram-negative bacterial suspensions and were analyzed in duplicate by a TaqMan-based qPCR assay based on the 16S rRNA sequence.

The effect on culturability of *X. fastidiosa*, generally increased over time for most of the tested peptides, with higher values obtained at 3 hours than at 30 minutes. The maximum

Funded by the European Union

population reductions at 30 min and 3 h were 4.77 logs and 5.5 logs, caused by peptides BP174 and 1036, respectively. In most cases, peptides presented a dose-effect relationship. Regarding the tested STs, ST6 of subsp. *multiplex* proved to be the most sensitive to the selected peptides while ST53 of subsp. *pauca* was the most resistant. The order of sensitivity of the STs was ST6 > ST1 and ST2 > ST7 > ST53. The most active peptides against most of the STs were BP178, followed closely by 1036 and BP473. As expected, Peps did not show any effect on the culturability or bactericidal activity. There seems to be a strong correlation between cell culturability and viability, indicating that the main mechanism of these peptides must be the disruption of the plasmatic membrane (lytic). However, there are some exceptions such as BP473 and HH15. For example, HH15 had a strong effect on the culturability of ST6, but it was not related to bactericidal activity, which was quite low.

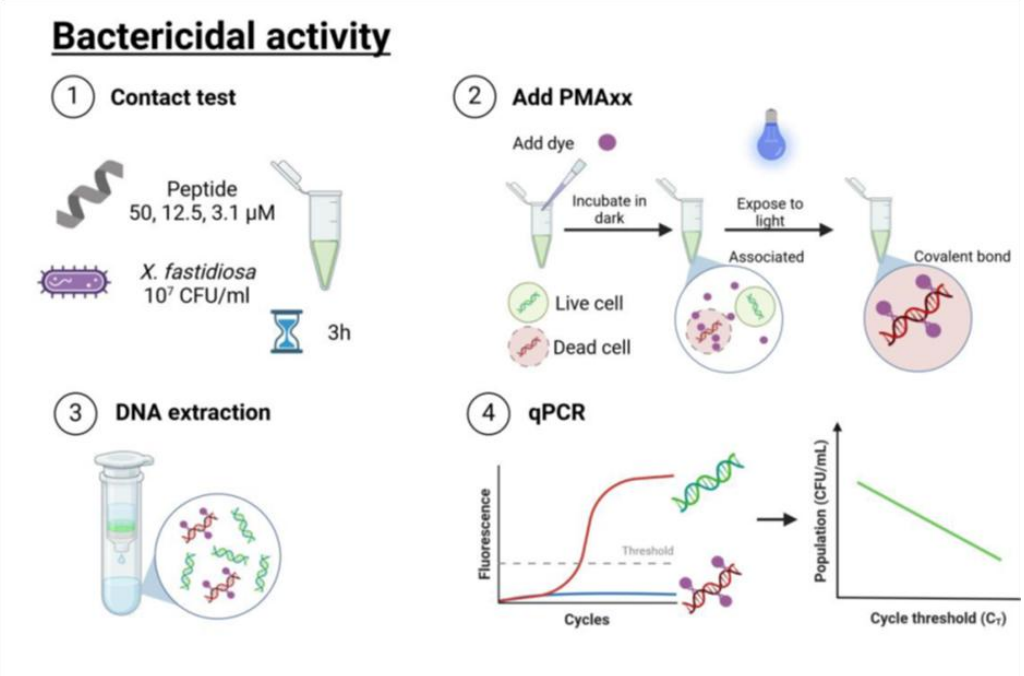


Figure 15: Assessment of the bactericidal activity of peptides using a contact test with determination of the time-course of cell survival by using a viability qPCR assay (Baró et al., 2020).

The bactericidal activity of the above mentioned peptides was confirmed by TEM and SEM microscopy (Figure 16). The observations revealed cell lysis and the formation of pores and membrane/envelope distortion as the possible cause of the bactericidal effect on *X. fastidiosa.*

Funded by the European Union

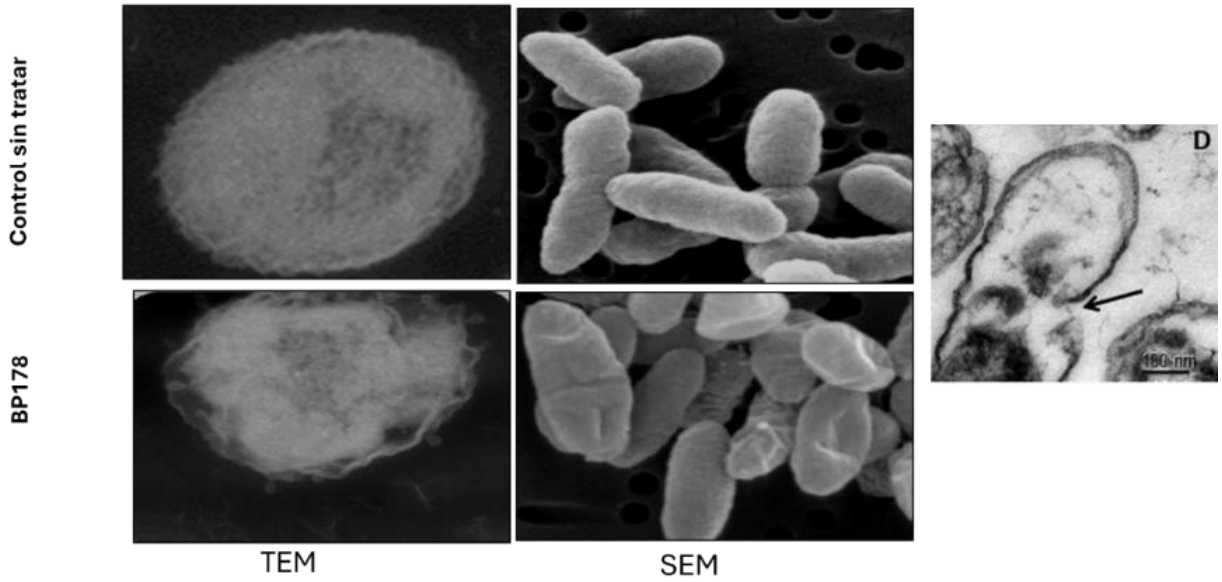


Figure 16: Electron microscopy micrographs made with TEM and SEM of the cells of *X. fastidiosa* untreated and treated with peptide BP178. In the right part a cell is shown with a cell envelope distortion and porus.

For antibiofilm activity, 20 µL of peptide at 50 µM were mixed with 180 µL of *X. fastidiosa* suspension (adjusted at an OD_{600} of 0.1) in PD3 in 96-well plates. Peptides that caused a population reduction >2.5 logs at 50 µM in the culturability test were tested at 3.1 µM to prevent the influence of their antimicrobial activity in the biofilm formation was estimated using the crystal violet assay (Zaini et al., 2009). Three replicates of 10 wells were prepared for each peptide and strain. The microplates were incubated at 28 °C under continuous shaking (120 rpm) for 5 days. Afterwards, planktonic cells were removed, the plates were rinsed gently with sterile distilled water two times and stained with 250 µL of crystal violet (0.1%) for 20 min. Then, excess dye was discarded by washing the plates two times with sterile distilled water. Finally, crystal violet adhered to the biofilm was solubilized with 250 µL of a mixture of ethanol/acetone (4:6) for 10 min and measure of OD595 was made.

Regarding the antibiofilm activity, the strain of ST1 was the most sensitive to the selected peptides, while strains of ST6 was the most resistant (Figure 17). The peptide with the broadest antibiofilm activity against the selected STs was BP178, which presented a biofilm formation ratio that oscillated between 0.21 and 0.61 against ST1, ST2, ST6 and ST7. Nevertheless, it did not show antibiofilm activity against the strain of ST53. It is interesting to note that peptides 1036 and BP473 presented high antibiofilm activity against ST53, which is of special relevance since it's the causal agent of Olive quick Decline Syndrome (OQDS) (Figure 17).

Funded by the European Union

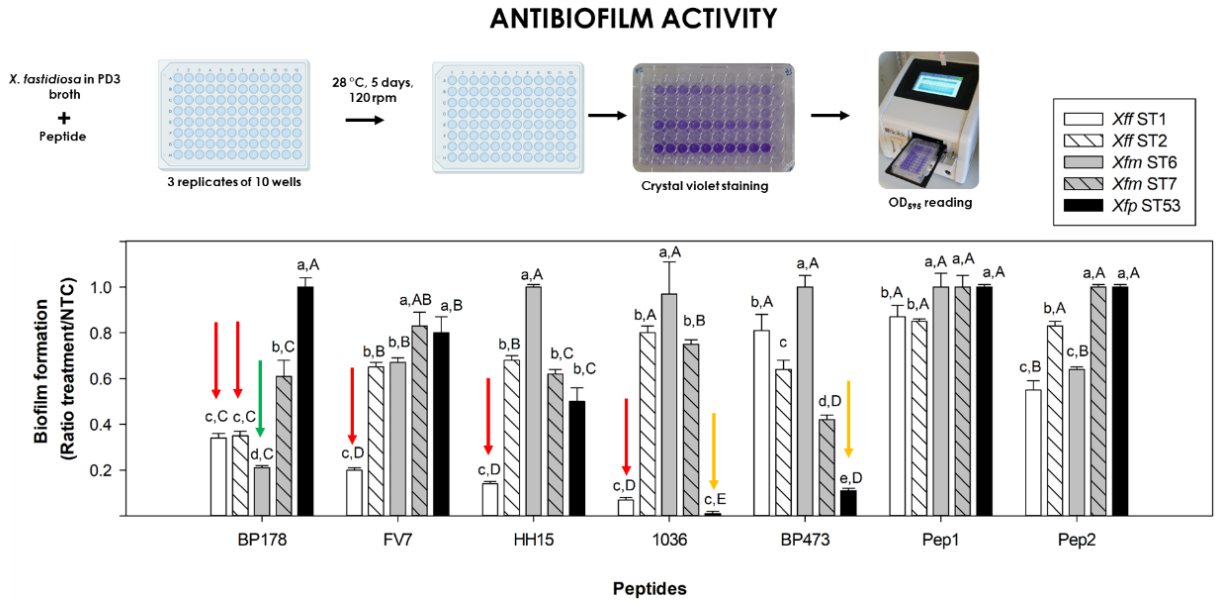


Figure 17: Measurement of antibiofilm activity of peptides against five STs of *X. fastidiosa* using the crystal violet microplate assay.

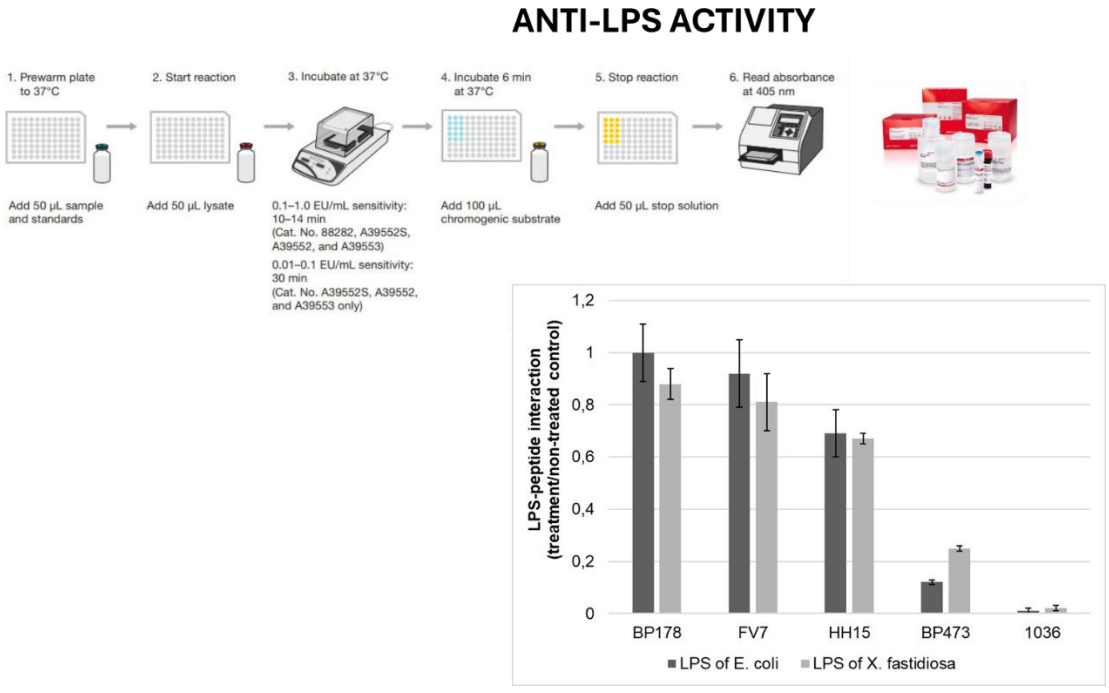


Figure 18: Assay of interaction of peptides with lipopolysaccharides from *Xylella fastidiosa* using the LAL toxicity assay with a standard of *E. coli* LPS.

Funded by the European Union

In addition to the previously reported activities, the capacity to bind the lipopolysaccharide (LPS) of *X. fastidiosa* was studied using a Limulus LPS-Peptide neutralization assays using the Pierce Chromogenic Endotoxin Quant Kit in 96-well plates with a lyophilized *E. coli* (O111:B4) endotoxin standard (from 0,1 to 1 EU/ml) and the optical density at 405 nm (OD_{405}) was measured (Figure 18). The degree of interaction was measured by the ratio (R) between OD_{405} of treatments (OD_T) and OD_{405} of the non-treated control (OD_{NTC}). From a set of peptides with bactericidal activity against X. fastidiosa, peptides BP473 (a lipopeptide) and peptide 1036 were strongly binding to LPS, whereas BP178 was not interacting (Figure 18).

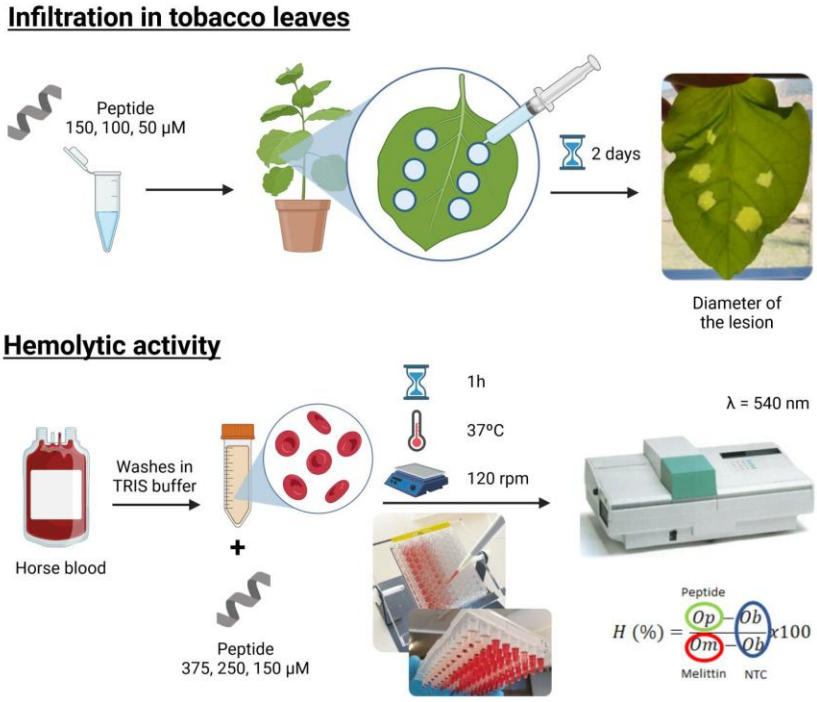
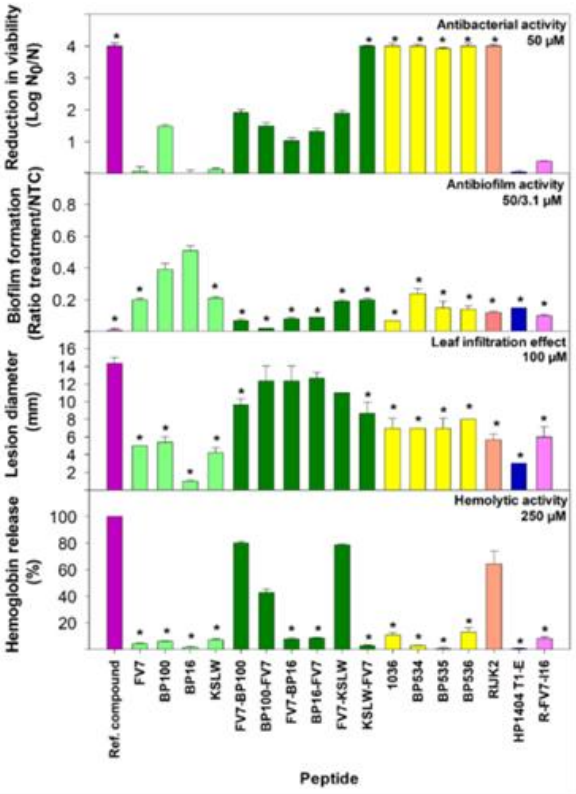


Figure 19: Procedures used for determination of the phytotoxicity of selected peptides by leaf infiltration in *Nicotiana tabacum*, and animal toxicity using hemolysis of horse red blood cells.

The toxicity of the best peptides was also studied using leaf infiltration in a plant model (*Nicotiana tabacum*) and the hemolytic activity with horse blood cells (Figure 19).

Figure 20 summarizes the results of bactericidal, antibiofilm, and toxicity of selected peptides. During BeXyl project, peptides with bactericidal and antibiofilm activity against *X. fastidiosa* and moderate toxicity have been identified. A PCA allowed to classify these peptides into four groups according to their distinct biological activity profile (Figure 20). An interesting group was composed by peptides 1036, RIJK2, and magainin 2 as they displayed dual activity (high bactericidal and antibiofilm activities) and moderate toxicity. Another group with many peptides displayed high antibiofilm activity, but low/moderate bactericidal activity and a low toxicity profile. Peptides 1036 and RIJK2, with dual activity against X. fastidiosa and moderate toxicity, would be the most promising ones as they may be able to simultaneously inhibit biofilm formation and kill *X. fastidiosa* cells (Figure 20).

Funded by
the European Union



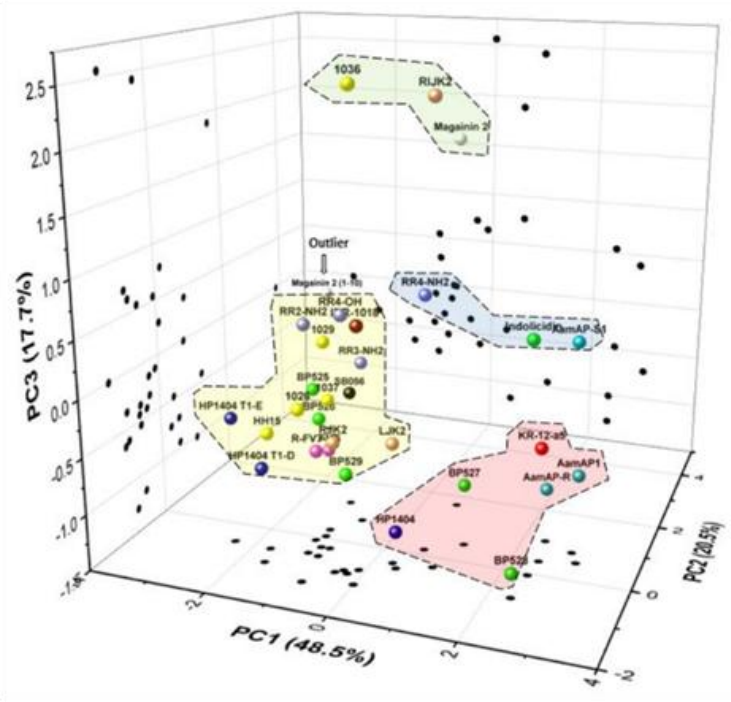


Figure 20: Bactericidal and antibiofilm activity against *Xylella fastidiosa* subsp. *fastidiosa* IVIA 5387.2, tobacco leaf infiltration effect, and hemolytic activity of peptides. The asterisk (*) indicates the peptides that have the best values for each activity according to the Duncan's test ($P < 0.05$). The reference (Ref.) compounds used were cecropin B for bactericidal activity, 1026 for antibiofilm activity, and melittin for tobacco leaf infiltration effect and hemolytic activity. For antibiofilm activity, peptides with very high bactericidal activity were diluted at 3.1 mM (KSLW-FV7, 1036, BP534, BP535, BP536, and RIJK2).

2.3.2. Screening *in planta* of selected single peptides

Nicotiana benthamiana was used initially as a model to test the effect of selected peptides in plant response by following the expression levels of defense-related genes in leaves (Figure 21). Afterwards, with the previous data *Prunus dulcis* cv. Avijor potted plants were used to confirm the results. All peptides were applied by endotherapy, each application consisted of three shots of 10 µl (30 µl of total peptide/plant) of a stock solution of peptides at 20 mM (BP178, BP473, FV7, HH15, and, 1036) and 100 µM for the endogenous peptides (PpPep1 and PpPep2) using a high precision microinjector (NanoJet, Chemyx, Stafford, TX, U.S.A.) provided with a Hamilton 250-µl syringe with a thin needle with bevel tip (Fisher Scientific, NH, U.S.A) (Figure 21 right). The needle end was introduced until approximately one half of the plant stem diameter to reach the vascular system. Nontreated controls were performed using water instead of the peptide solution. The injections were performed on the same side of the stem in a section of 3 cm at around 15 cm above the substrate level (Figure 22).

Funded by the European Union



Figure 21: (Left pictures) Quarantine greenhouse at the University of Girona facility (P2+ level) and conditions of work. (**Right pictures**) Microinjection device for inoculation of *X. fastidiosa* suspensions and for treatment with peptides.

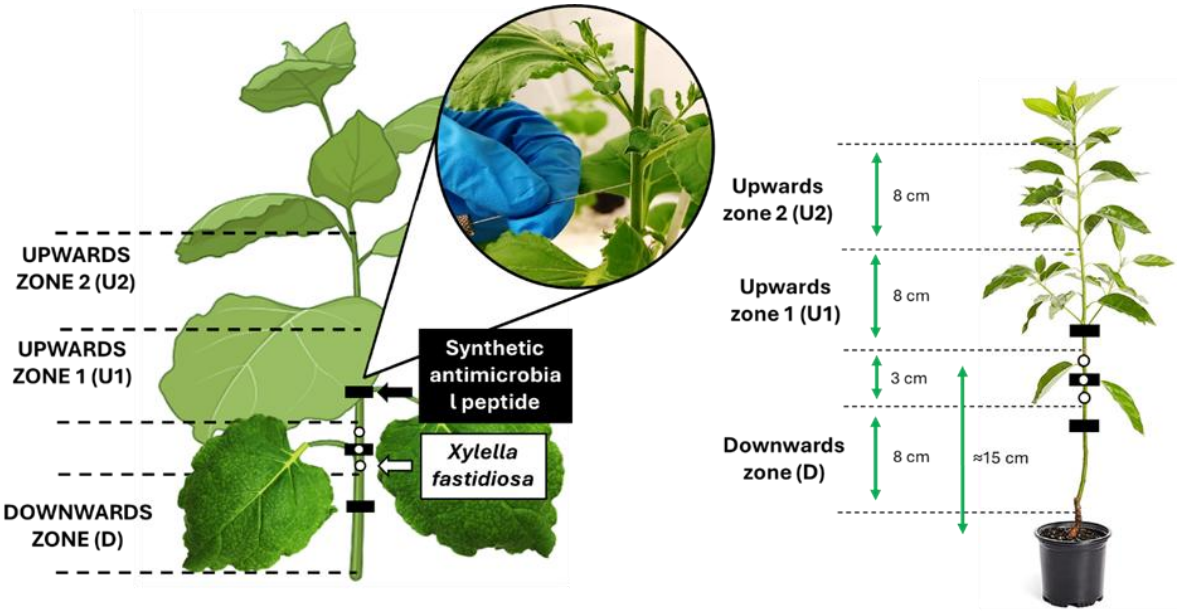


Figure 22: Inoculation points for *Xylella fastidiosa* (white circles) and application points of the synthetic antimicrobial peptides (black rectangle) in *Nicotiana* and almond plants. Sampled zones are also indicated as upwards zones 1 and 2 and downwards zone.

Funded by
the European Union

2.3.2.1. Nicotinana benthamiana *as a model to screen peptides against* Xylella fastidiosa

Transient expression of genes encoding peptides BP134 and BP178 by means of a Potato virus X (PVX) based-vector system, and treatment with synthetic peptides by endotherapy, were evaluated in the control of *X. fastidiosa* infections, in the model plant *Nicotiana benthamiana* (Figure 23). Transient production of BP178 significantly decreased disease severity compared to PVX and nontreated control (NTC) plants, without adverse effects. Plants treated with synthetic BP134 and BP178 showed consistently lower levels of disease than NTC plants. However, the coinfection with PVX-BP134 and *X. fastidiosa* caused detrimental effects resulting in plant death. The levels of *X. fastidiosa* in three zones sampled, upwards and downwards of the inoculation/treatment point, significantly decreased compared to the NTC plants, after the treatment with BP178, but not when BP178 was produced transiently (Figure 23). The effect of treatment and transient production of BP178 in the induction of defense-related genes was also studied.

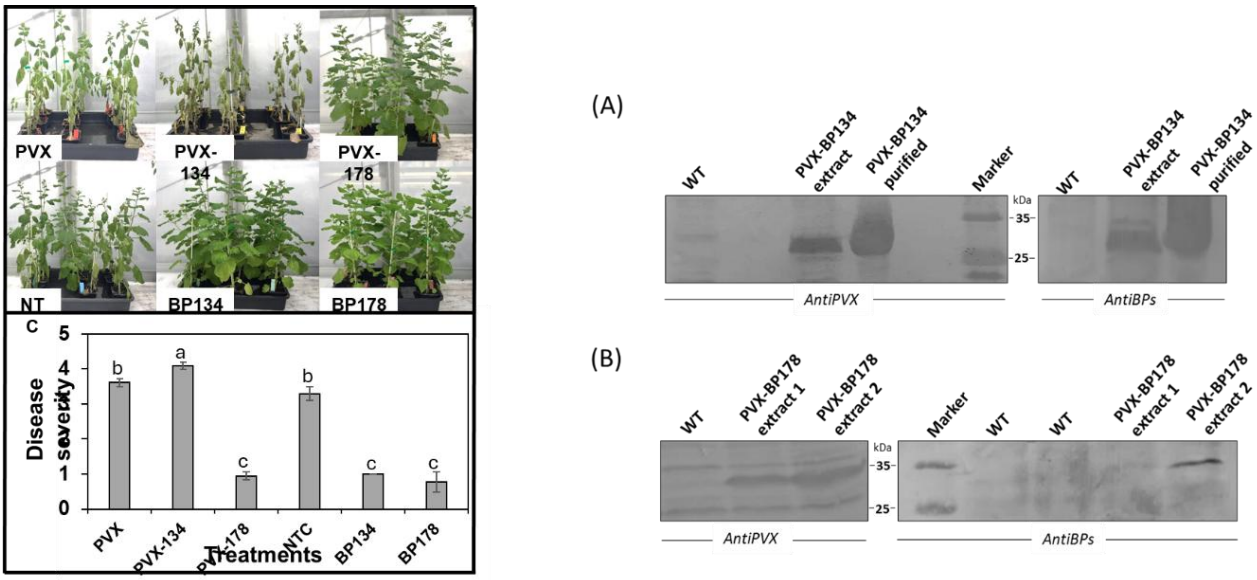


Figure 23: (Left figure) Effect of endotherapy with BP178 or BP134, and by heterologous production of the peptides on *Xylella fastidiosa* infections in *Nicotiana benthamiana* plants. The treatments were: PVX, empty vector; PVX-134, vector with BP134 gene; PVX-178, vector with BP178 gene; BP134, synthetic peptide; BP178, synthetic peptide; and NTC, non-treated control. Different letters between treatments correspond to statistically significant differences between treatments (Tukey's test, P ≤0.05). **(Right figure**) Western immunoblot analysis of PVX CP-BP134 and PVX CP-BP178 fusion proteins in total protein extracts from *N. benthamiana* leaf tissues. WT indicates protein extracts from leaves of non-transfected plants. (A) Extracts from PVX-BP134 and WT lines. Purified viral particles of PVX CP-BP134 were also analyzed. (B) Extracts from PVX-BP178 lines 1-2 and WT line. Immunodetection was performed using specific polyclonal anti-BP178/antiBP134 or antiPVX antibodies and NBT/BCIP colorimetric detection by alkaline phosphatase-conjugated antibodies.

Funded by the European Union

To analyze gene expression in treated *N. benthamiana* plants, a quantitative real-time PCR (qPCR) was carried out in a fluorometric thermal cycler (qPCR Quant Studio 5) by using SYBR® Green PCR Master Mix. For each gene system, the concentration of the primer pair was optimized to prevent non-specific reactions or artefacts that could hide the results, and the linearity within a range of number of copies of each gene was evaluated as well as the efficiency for each curve was calculated (efficiencies ranging from 80 to 98.8 %, $R^2 \geq 0.98$). Melting curve analysis was performed after each amplification to verify amplification specificity. A constitutive gene (actin gene) was used as reference control. Relative quantification of gene expression was done using $\Delta\Delta C_T$ method, and the relative expression values were normalized against the actin gene as an internal control. The gene expression of 12 genes related to *N. benthamiana* plant defense pathways was quantified. The statistical significance of the gene expression data was determined using the REST2009 Software. Expression levels higher than 1.5-fold change were considered differentially expressed.

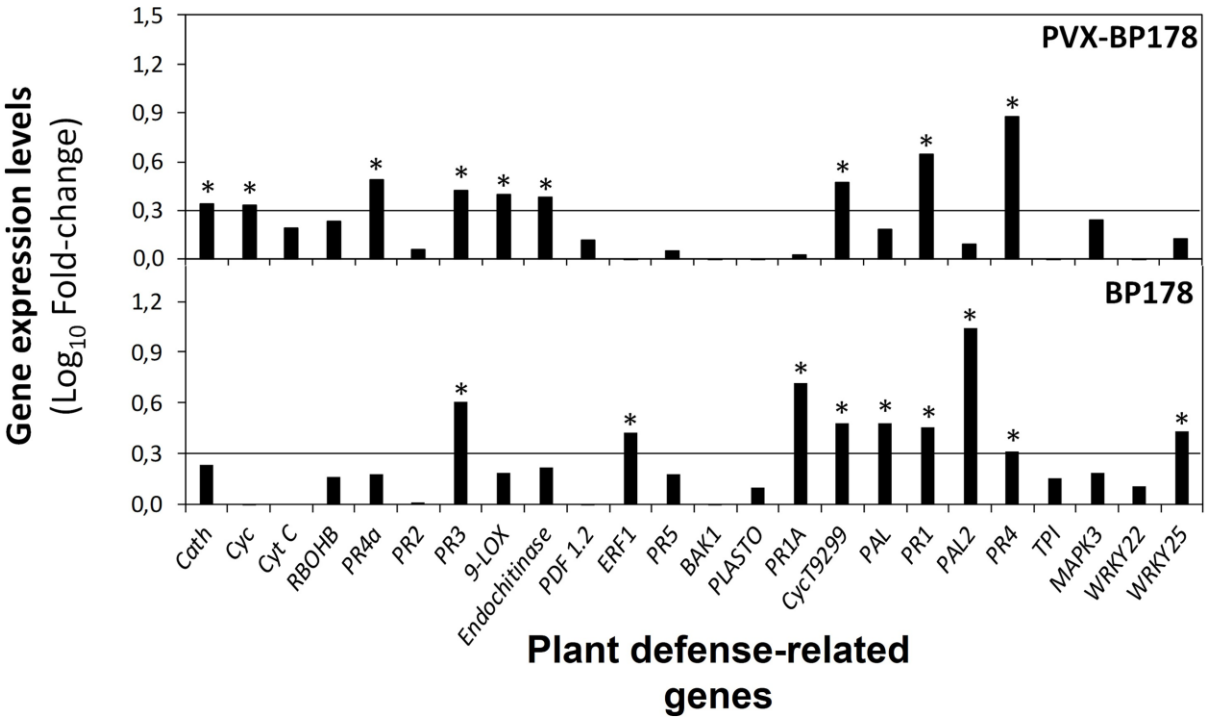


Figure 24: Expression levels of defense genes in *Nicotiana benthamiana* plants in response to endotherapy with synthetic BP178 or transient expression with PVX-BP178, using RT-qPCR analysis. Black line, cut-off values for genes with > 2-fold change value (log10, 0.3) (Relative quantification method using DDCT method). Each BP178 treatment was compared to its appropriate control (i.e., PVX-BP178 compared to PVX control; BP178 applied by endotherapy compared to non-treated control plants, where plants were treated with water by endotherapy). Asterisks indicate significant values of fold-change.

Funded by the European Union

Synthetic BP178 applied by endotherapy induced the expression of ERF1, PR1a, PAL, PALII and WRKY25, while the transient expression of BP178 overexpressed the Cath, Cyc, PR4a, 9-LOX and Endochitinase B genes. Both treatments upregulated the expression of PR1, PR3, PR4 and CycT9299 genes compared to the NTC or PVX plants (Figure 24). It was concluded that the effect of BP178, either by endotherapy or by transient expression, on the control of the *X. fastidiosa* infections in *N. benthamiana*, was due in part to the induction of the plant defense system in addition to its bactericidal activity reported in previous studies. However, the protection observed when BP178 was transiently produced seems mainly mediated by the induction of plant defense, because the levels of *X. fastidiosa* were not significantly affected.

2.3.2.2. *Screening of peptides in almond* (Prunus dulcis)

A series of experiments were performed with almond (cv. Avijor) potted plants in the greenhouse to both determine the effect of selected peptides in controlling population levels of *X. fastidiosa* and disease, and to know the type of response of the plant host to the peptide. Inoculation and treatments were performed by microinjection as described previously.

In a first stage one of the peptides, BP178, applied by microinjection into almond plants was monitored into the xylem at a distance from application (U1 position), using Western analysis with a specific antibody. It was confirmed that the peptide was detected until 60 days post treatment at significant and effective concentrations (Figure 25).

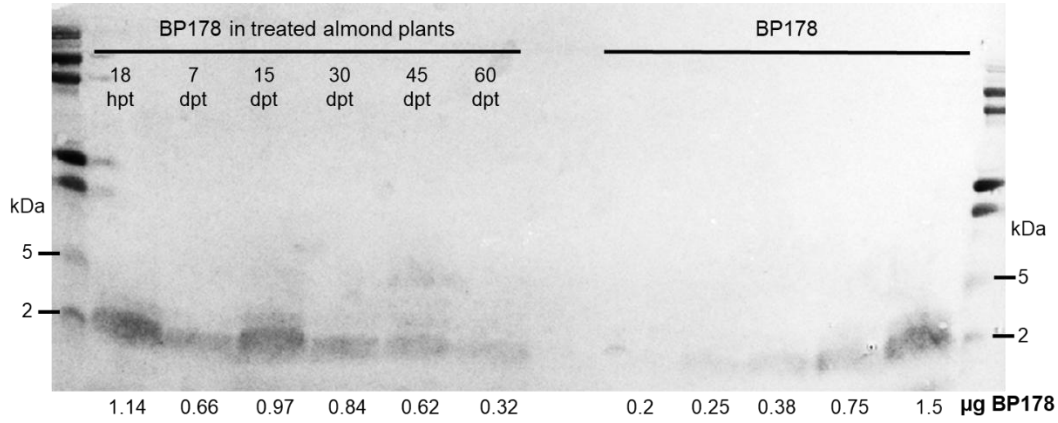


Figure 25: Western blot analysis of the xylem sap of cv. Avijor, *Prunus dulcis* almond, potted plants after endotherapy with peptide BP178. The analysis was performed at different days. On the right standard concentrations and molecular markers.

The population levels of viable *X. fastidiosa* cells (v-qPCR) in almond plants of cultivar Avijor were determined after the treatment with BP178 by endotherapy, following the strategies including preventive (1 day before the pathogen inoculation), curative (3 and 7 dpi), and the combination of both treatments, and compared with a nontreated control (NTC) (Figure 26).

Funded by the European Union

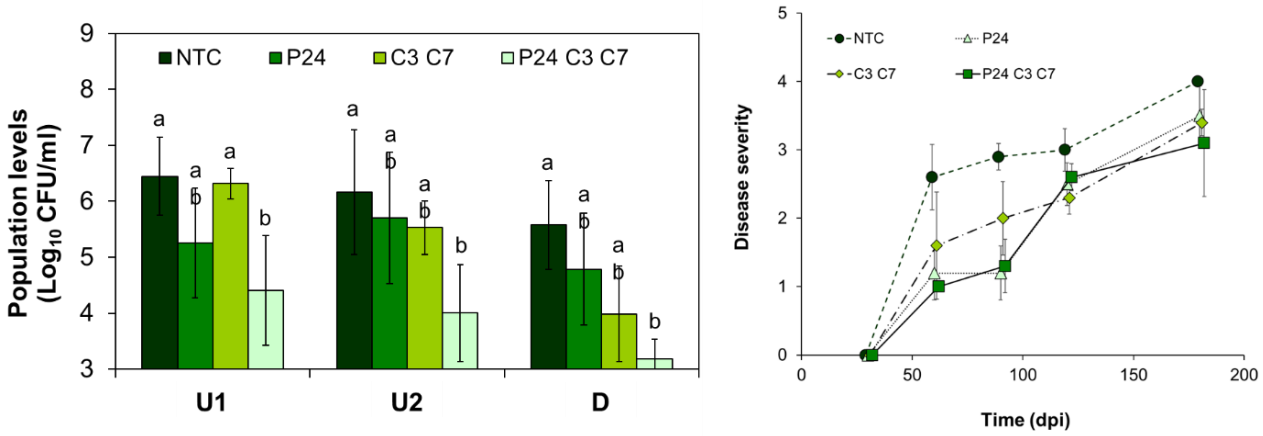


Figure 26: Effect of BP178 treatments on viable *Xylella fastidiosa* subsp. *fastidiosa* IVIA 5387.2 population levels in sap of almond plants at 30 days post-inoculation (dpi). The treatments were preventive (1 day before inoculation), curative (3 and 7). Disease severity of almond leaf scorch in plants treated with BP178 using different strategies compared with a nontreated control over a period of 180 days post-inoculation (dpi) of *X. fastidiosa*.

The combined treatment was the most effective one in reducing the viable cells of *X. fastidiosa* in sap, with a decrease between 2 and 3 log in all plant parts analyzed, compared with NTC. The preventive or curative treatments when used independently did not significantly reduce the population levels. The disease severity was also evaluated over a period of 180 dpi (Fig. 3). Symptoms started between 30 and 60 dpi. NTC plants were the most affected ones during the whole experiment, with almost half of the leaves showing marginal necrosis already at 60 dpi. Disease severity increased over time and plants showed leaf scorch symptoms and experienced a progressive decline at 180 dpi. In plants treated with BP178, ALS infection was reduced during the first 120 dpi compared with the NTC, being the group of plants preventively treated with BP178 (preventive and combination treatments) the ones showing the lowest disease intensity (60 to 65% of disease severity reduction compared with the NTC, at 60 and 90 dpi) (Figure 26). Additional experiments were performed with other peptides obtaining similar results (Figure 27).

The effect of BP100 on the xylem vessels of infected almond plants was assessed at 90 dpi. As expected, the xylem vessels of the plants treated with BP100 showed differences when compared with the not-inoculated control and the NTC (Figure 28). The not-inoculated plants did not show biofilm-like structures but exhibited a few small tyloses attached to the walls in 4 ± 1.2% of xylem vessels. Most of the xylem vessels found in the inoculated plants (NTC) showed biofilm-like structures (87.1 ± 1.4%), presence of tyloses, or a combination of both and also showed vessels that were partially or completely occluded. Xylem vessels of plants treated with BP100 were similar to the not-inoculated plants and showed only a 34.3 ± 1.3% of xylem vessels affected with biofilm-like structures.

Funded by the European Union

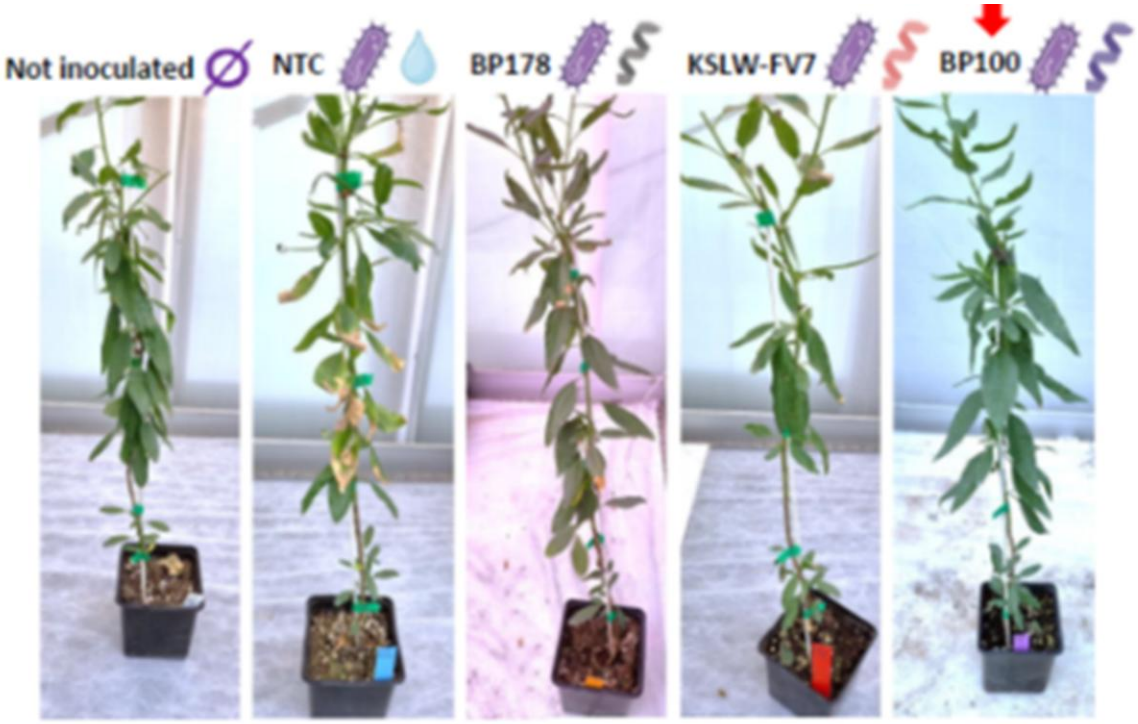


Figure 27: Symptoms of almond leaf scorch in almond cv. Avijor plants after inoculation with *Xylella fastidiosa* and treatment with different functional peptides (BP178, KSLW-FV7, BP100). NTC: Non-treated control.

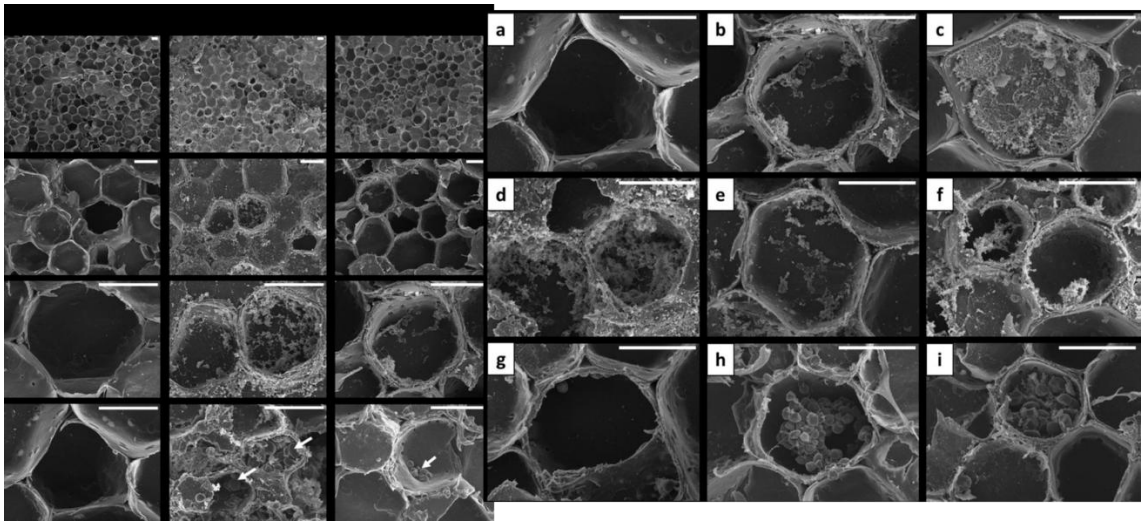


Figure 28: Representative scanning electron micrographs of xylem vessels of *Prunus dulcis* plants that were not inoculated, inoculated with *Xylella fastidiosa* (not-treated control [NTC]), or inoculated with *X. fastidiosa* and treated with the peptide BP100. The white scale bar corresponds to 20 mm in all of the images. White arrows indicate tyloses formation.

Funded by
the European Union

To study the effect of BP178 on the transcriptome of almond plants eight mRNA libraries were sequenced from four replicates of *P. dulcis* 'Avijor' treated with BP178 and four replicates of NTC. Each library had approximately 15 million raw reads that, after filtering for high quality reads, 13 to 14 million sequences were kept. Reads were assigned to the *P. dulcis* reference genome (Sánchez-Pérez et al. 2019), and between 75 and 77% of them were uniquely mapped to genes. The quality of the experiment was assessed using a principal component (PC) analysis. PC2 accounted for 24.2% of the total variation in the dataset, which resulted in two clusters that clearly separated treated from nontreated plants. After bioinformatics analysis (Figure 29), differentially expressed genes (DEGs) were identified, which after filtering resulted in 97 upregulated and 105 downregulated genes.

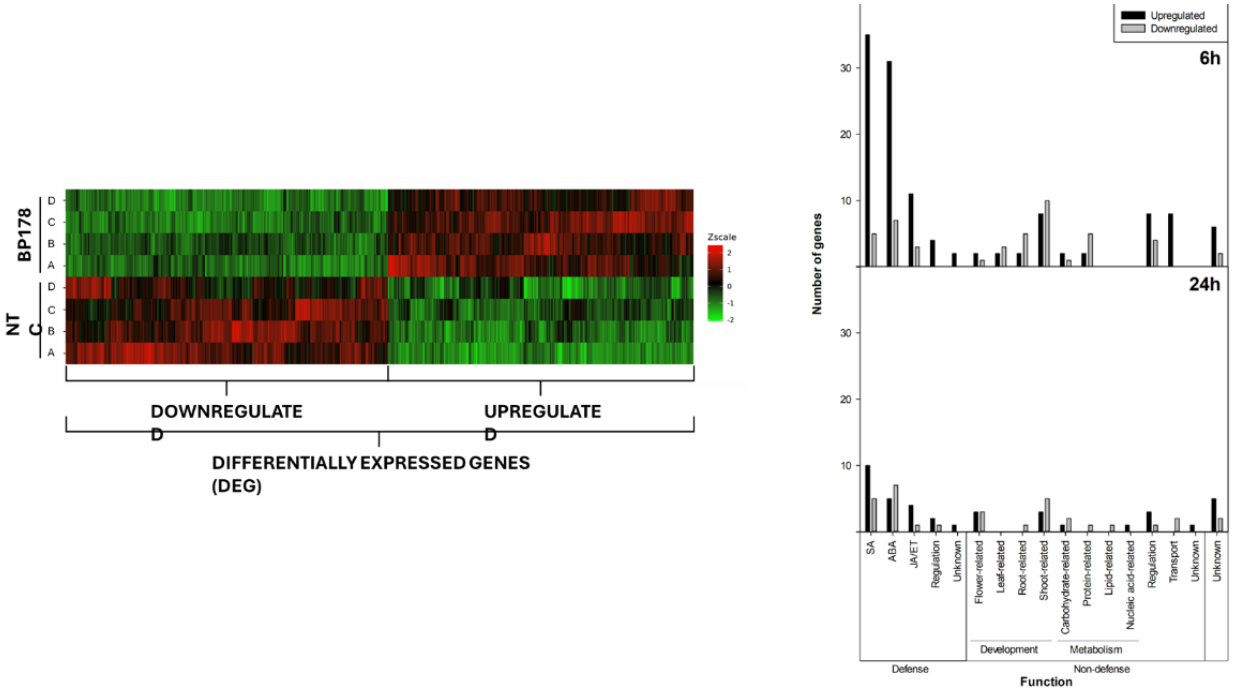


Figure 29: (Left figure). Heat map of the expression patterns (Z-scaled fragments per kilobase million values) of the differently expressed genes (DEGs) in almond plants (replicates A, B, C, and D) that were treated with the peptide BP178 compared with the nontreated control (NTC). Columns correspond to the identified DEGs. Changes in expression levels are displayed from green (under expressed) to red (overexpressed). The order of genes was established after hierarchical clustering using the Euclidean distance. **(Right figure)**. Number of differentially expressed genes (upregulated and downregulated) in almond plants due to BP178 treatment classified by function (major defense and nondefense pathways).

BP178 peptide presented the ability to upregulate several genes such as ERF1 (Ethylene transcription factor) that is involved in the ethylene and jasmonate pathway, which encodes a transcription factor that regulates the expression of pathogen response genes that prevent disease progression LOX (Lypoxygenase) that is overexpressed by the jasmonic pathway and

Funded by the European Union

signals in wounds, pathogen attack and promotes cell death (Baró *et al*. 2022), PR1 (pathogenesis-related genes) PR3 (Endochitinase) and PR2 (Glucanase) all of them involved in signaling by pathogen attack by salicylic acid pathway, MAPK3 (Mitogen-activated protein kinase 3) which play a central role in PAMP-triggered immunity. Following PAMP perception, many pattern recognition receptors have been found to activate specific MAPK signals to elicit the defense response, and PAL (PHE ammonia lyase) which participates in the synthesis of SA. Another peptide that stood out was HH15, showing high overexpression of all PR genes (PR3, PR1, PR2, PR4a and PR4a, pathogenesis-related genes). The HH15 peptide showed overexpression results well above the BP178 peptide, showing itself as a very good candidate to achieve the objective of *priming* plants.

Priming plants with BP178 induced defense responses mainly through the salicylic acid pathway, but also overexpressed some genes of the jasmonic acid and ethylene pathways (Figure 30).

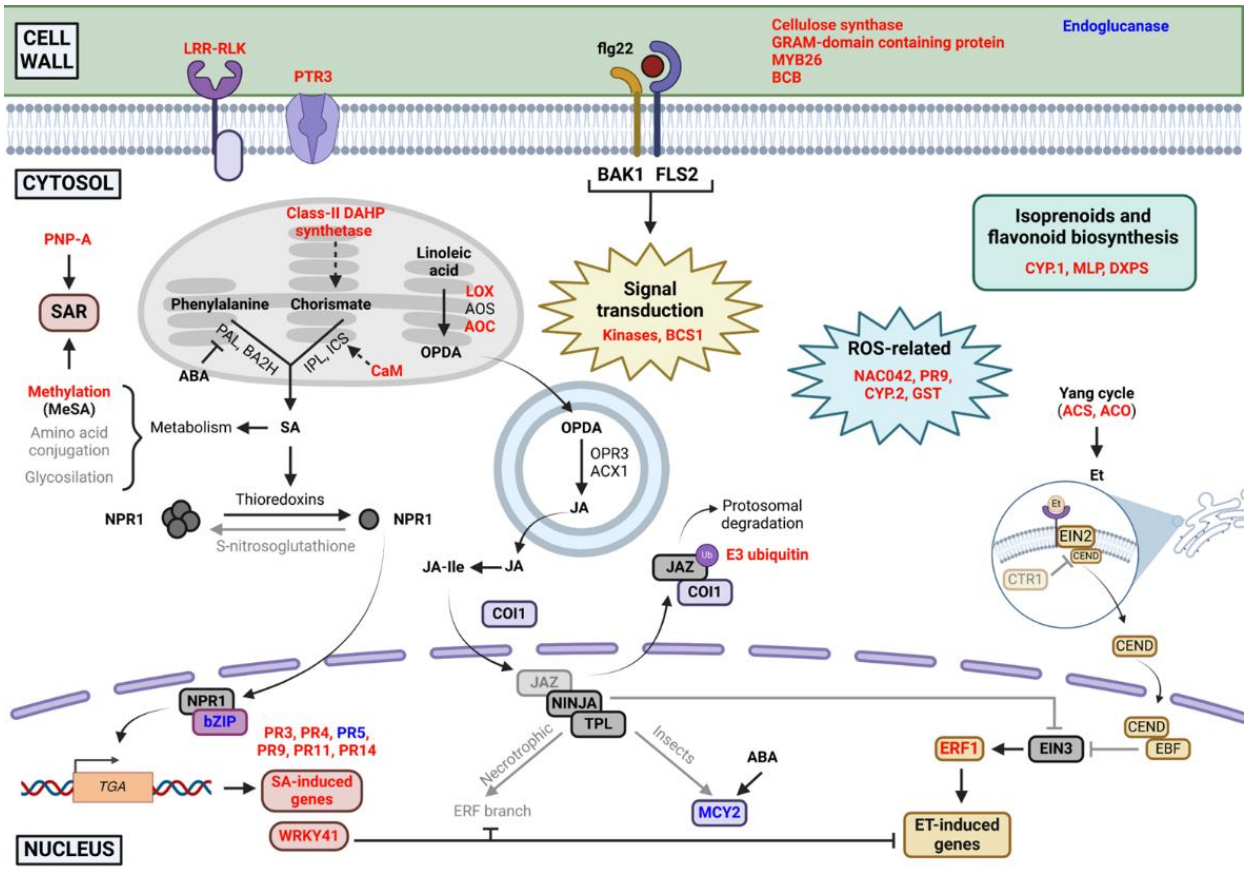


Figure 30. Model of the major plant defense pathways. Expression of the proteins of each pathway that have been affected by the treatment of BP178 after 24 h are highlighted. Red names correspond to upregulated genes and blue names to downregulated genes. Names in black correspond to proteins that are participating in the pathway. Image created with BioRender (https://biorender.com).

Funded by the European Union

During the different studies new defense elicitor peptides have been identified which control *X. fastidiosa* infections in almond (Figure 31). A library of peptides that includes BP100-flg15, HpaG23, FV7, RIJK2, PIP-1, Pep13, BP16-Pep13, flg15-BP100 and BP16 triggered a stronger defense response in almond plants than flg22-NH2. Peptides induced different gene expression profiles that could be clustered into five groups related with their transcriptomic pattern. BP100-flg15, HpaG23, FV7, RIJK2, and PIP-1 (group 2) and Pep13, BP16-Pep13, flg15-BP100, and BP16 (group 3) led to a higher gene expression than the peptides of other groups. Interestingly, group 2 led to the upregulation of all genes and exhibited an expression intensity ranging from 12 to 17. Group 3 displayed an expression intensity ranging from 13 to 18, and had a high overexpression of the genes *PR3, CYP.1, GST, PR9,* and *RLK*. Peptides BP16-KSLW, BP16-flg15, flg15- OH, BP100, Pep13-BP16, flg15-BP16, elf18-NH2, flg22- OH, KSLW-FV7, csp15, BP13, elf18-OH, and flg22-NH2 (group 1) exhibited an expression intensity ranging from 8 to 16. Among them, BP16-KSLW, BP100, Pep13-BP16, and flg15-BP16 induced a high upregulation of at least four genes, such as *PR3, CYP.1, GST,* and *DNAJ*. KSLW (group 4) exhibited an expression intensity of 12 and caused a high upregulation of *DXPS*, *PR3*, *CYP.1,* and *RLK*. Finally, 1036 and KSLW-BP100 (group 5) only caused a high upregulation of PR3 and CYP.1 and displayed an expression intensity ranging from 4 to 5 (Figure 31).

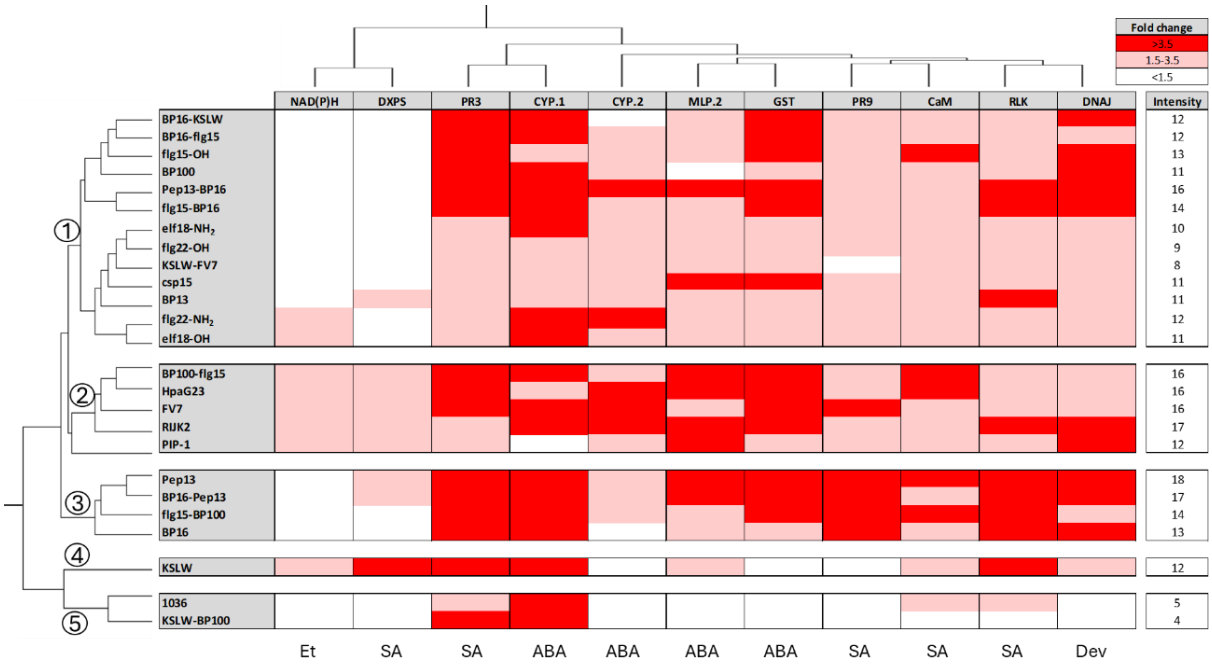


Figure 31: Heat map of the expression pattern of marker genes in almond plants after 6 h of the treatment with different peptides applied by endotherapy at 20 µM. Rows correspond to peptides and columns correspond to genes. The order of the peptides and the genes was established after hierarchical clustering using the Euclidean distance. Genes are colored depending on the intensity of upregulation caused by the treatment with the indicated peptide. Values are the means of three replicates of three plants each. Intensity of expression is represented as a numeric value that corresponds to the sum of the intensity of upregulation which for each gene is 0 when < 1.5-fold change, 1 when 1.5–3.5 and 2 when > 3.5.

Funded by the European Union

Based on the above-mentioned studies including the *in vitro* testing against different subspecies of *X. fastidiosa* and with a large library of peptides and on the *in planta* assays of selected members of the library in *N. benthamiana* and *Prunus dulcis* (cv. Avijor), the peptides listed in Figure 32 we considered the best. These peptides were BP178, 1036, KSLW-FV7, BP100, FV7, and flg22-NH2 (Figure 32). Attending the amino acid sequence or hypothetical structure it was not possible to find a relationship among them (Figure 33).

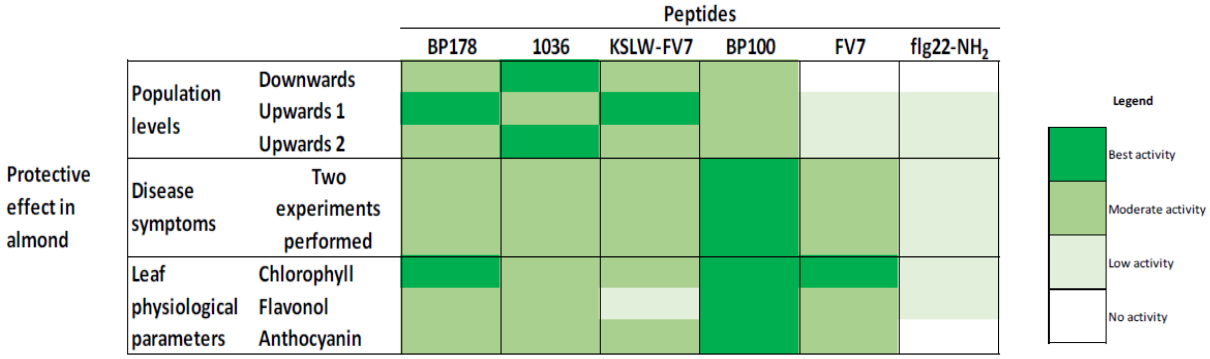


Figure 32: An overview of the characteristics of the best peptides that have been selected from the in vitro and in planta studies for control of *X. fastidiosa* in *N. benthamiana* and almond.

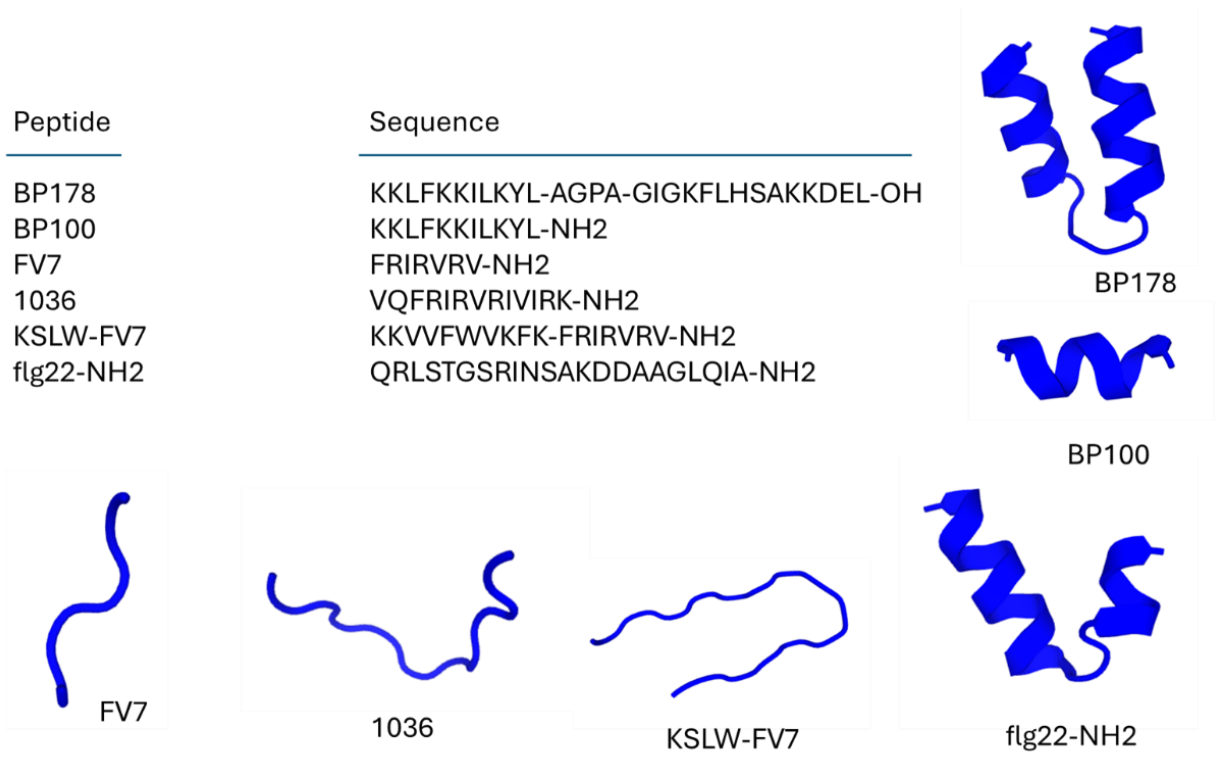


Figure 33: Amino acid sequences and hypothetical structures according to the PEPFOLD-3 software of the best peptides that have been selected from the in vitro and in planta studies for control of *X. fastidiosa* in *N. benthamiana* and almond.

Funded by the European Union

2.3.3. Screening of random peptide mixtures

Three different **random peptide mixtures (RPMs)** were synthesized to be tested for anti-*X. fastidiosa* activity. These RPMs include the following: (1) LK20, a 20-mer peptide composed of lysine and leucine; (2) FK20, a 20-mer peptide composed of lysine and phenylalanine; and (3) P-FK5, a 5-mer peptide composed of lysine, phenylalanine and palmitic acid. To test their activity, peptides were added to *X. fastidiosa* cultures (in PD3) in microtiter plates at concentration of 20, 20, 80, 100 and 200 µg/mL and incubated at 28˚C. OD600 was measured 7 and 12 days after initiation (dai) and serial dilution plating was also done at the same time points. Based on OD measurements, we observed significantly reduced *X. fastidiosa* growth with the pFK5 peptide (at 200 µg/mL) 7 dai and with the LK20 peptide at 100 and 200 µg/mL 12 dai. Unfortunately, the CFU count results were inconsistent and no conclusions could be reached.

The effect of RPMs on *X. fastidiosa* growth and biofilm formation was reassessed using a different setup involving glass test tubes. Each test tube contained 0.5 mL of PD3 medium, to which *X. fastidiosa* inoculum (OD_{600} ~ 1.5) was added. *X. fastidiosa* growth was evaluated by serial dilution and plating on PD3 agar plates three days after inoculation. Biofilm formation was assessed at 7 days after inoculation (dai). This experiment was repeated twice.

In both experiments, none of the tested RPMs inhibited *X. fastidiosa* growth or suppressed biofilm formation. In fact, some RPMs appeared to have the opposite effect. For example, LK20 promoted *X. fastidiosa* growth at concentrations of 40, 100, and 200 µM, while FK20 enhanced both growth and biofilm formation at 100 and 200 µM. A representative image and graph illustrating the results for FK20 are presented in Figure 34.

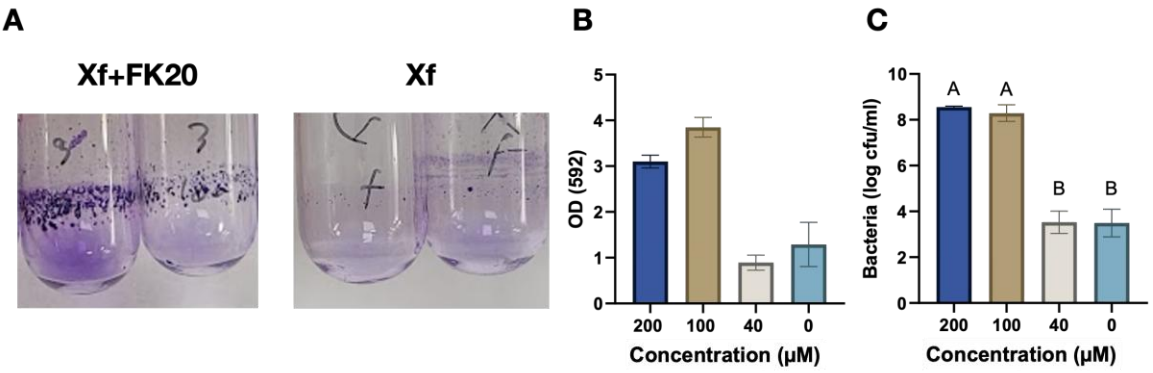


Figure 34: Effect of Random Peptide Mixtures (RPMs) on *Xylella fastidiosa* growth and biofilm formation. FK20, a 20-mer peptide composed of lysine and phenylalanine, was added to PD3 medium in which *X. fastidiosa* was grown. *X. fastidiosa* biofilm formation was examined 7 days after media inoculation by the crystal violet staining (**A**) and by measuring crystal violet absorbance following resuspension in ethanol (**B**). *X. fastidiosa* growth was measured 3 days after media inoculation by serial dilution and plating on PD3 agar plates (**C**).

Funded by the European Union

In summary, the effects of the different RPMs on *X. fastidiosa* growth and biofilm formation varied across experiments and were not consistent, making it difficult to draw definitive conclusions. However, considering all the experimental data, we can conclude that none of the tested RPMs had a significant inhibitory effect on *X. fastidiosa* growth or biofilm formation. On the contrary, under certain conditions, some appeared to enhance these traits. These findings suggest that the tested RPMs are unlikely to be effective candidates for *X. fastidiosa* control.

2.4. Bacteriophages

2.4.1. Characterization of a collection of phages

The whole genome sequencing of 19 selected phages, with high *in vitro* activity against *X. fastidiosa* strains, was performed. The general characteristics of the phage genomes are summarized in Table 1. BLAST analysis of the *de novo* genomes against the 'nt' database of the NCBI showed that the phages exhibited homology with sequences available in the GenBank database, with high (≥80%) coverage and identity. A wide diversity was obtained: nine phages belong to *Pradovirus* genus, six phages to *Alphatectivirus*, one to *Bosavirus*, one to *Salvovirus* and tow remain unclassified. Complementary analyses using Abricate showed no presence of virulence or antibiotic resistance genes. Furthermore, all analyzed phages by using PhageIA exhibited a lytic life cycle, indicating the absence of a genomic integration phase in bacterial hosts.

To determine the phylogenetic relationships of the phages, two sequences from different species within each genus resulting from the Blastn analysis were selected. Additionally, two representative sequences from the most closely related genera within the same viral family were included to enhance classification inference. Whole-genome sequence comparisons conducted using VIRIDIC allowed the classification of phages into various taxonomic ranks. Species demarcation was based on a threshold of 95%, while genus demarcation followed the 70% threshold, in accordance with the recommendations of the International Committee on Taxonomy of Viruses (ICTV). Phage isolates with MAFFT alignment scores exceeding 95% were grouped together. In Figure 35, a single representative was selected for each group: ViSe_6 represents ViSe_7, ViSe_8, ViSe_9, and ViSe_17; ViSe_10 represents ViSe_15 and ViSe_18; ViSe_22 is represented by a phage denominated ViSe_23; and ViSe_35 represents ViSe_33 and ViSe_34. ViSe_2 formed an independent species cluster because its intergenomic similarity with other phages was below 95%. Phage ViSe_4 clustered with members of the *Salvovirus* genus; however, the highest intergenomic similarity observed was 91.1%, indicating that this phage represents a distinct species within the genus. Phages ViSe_6, ViSe_7, ViSe_8, ViSe_9, ViSe_10, ViSe_14, ViSe_15, ViSe_17 and ViSe_18 were grouped within the genus *Pradovirus* as distinct species, exhibiting intergenomic similarities ranging from 68.2% to 94.7% among themselves.

To refine the classification of *Autographiviridae* phages following ICTV recommendations, an additional maximum likelihood phylogeny was constructed using the

Funded by the European Union

sequences of the DNA-dependent RNA polymerase and applying the GTR+G substitution model. This analysis supported previous evidence that some of the phages cluster within the *Pradovirus* genus, with high similarity to reference sequences (bootstrap support of 95–100). Specifically, phages ViSe_6, ViSe_10, and ViSe_14 grouped with NC 022987 and MK903278. In contrast, other phages formed distinct clades with strong bootstrap support (96–100), suggesting that they constitute new genera: ViSe_21 formed a distinct group with MT951568 and NC 022982, and ViSe_23 grouped with LR778216 in an independent lineage.

Table 1: General features of 19 sequenced phage genomes, including genome size, GC content percentage, number of coding sequences (CDS) and taxonomic classification.

Phage	Size (bp)	%GC	CDS	Class	Family	Genus
Xylella_phage_ViSe_2	63,992	66.4	95	*Caudoviricetes*	*Mesyanzhinovviridae*	*Bosavirus*
Xylella_phage_ViSe_4	55,215	63.0	77	*Caudoviricetes*	*Casjensviridae*	*Salvovirus*
Xylella_phage_ViSe_6	43,592	63.0	57	*Caudoviricetes*	*Autographiviridae*	*Pradovirus*
Xylella_phage_ViSe_7	43,477	62.9	57	*Caudoviricetes*	*Autographiviridae*	*Pradovirus*
Xylella_phage_ViSe_8	43,550	62.8	59	*Caudoviricetes*	*Autographiviridae*	*Pradovirus*
Xylella_phage_ViSe_9	43,466	62.9	56	*Caudoviricetes*	*Autographiviridae*	*Pradovirus*
Xylella_phage_ViSe_10	43,780	62.9	60	*Caudoviricetes*	*Autographiviridae*	*Pradovirus*
Xylella_phage_ViSe_14	43,606	62.8	56	*Caudoviricetes*	*Autographiviridae*	*Pradovirus*
Xylella_phage_ViSe_15	43,377	62.8	55	*Caudoviricetes*	*Autographiviridae*	*Pradovirus*
Xylella_phage_ViSe_17	43,579	63.0	57	*Caudoviricetes*	*Autographiviridae*	*Pradovirus*
Xylella_phage_ViSe_18	43,342	62.7	58	*Caudoviricetes*	*Autographiviridae*	*Pradovirus*
Xylella_phage_ViSe_21	42,782	60.5	61	*Caudoviricetes*	*Autographiviridae*	Unclassified
Xylella_phage_ViSe_22	41,733	58.1	55	*Caudoviricetes*	*Autographiviridae*	Unclassified
Xylella_phage_ViSe_33	14,926	48,2	31	*Kalamavirales*	*Tectiviridae*	*Alphatectivirus*
Xylella_phage_ViSe_34	14,926	48,2	31	*Kalamavirales*	*Tectiviridae*	*Alphatectivirus*
vB_Xf_IVIA-DoCa15	14,927	48,17	31	*Kalamavirales*	*Tectiviridae*	*Alphatectivirus*
vB_Xf_IVIA-DoCa18	14,798	48,18	31	*Kalamavirales*	*Tectiviridae*	*Alphatectivirus*
vB_Xf_IVIA-DoCa19	14,974	48,38	31	*Kalamavirales*	*Tectiviridae*	*Alphatectivirus*
vB_Xf_IVIA-DoCa21	14,825	47,41	31	*Kalamavirales*	*Tectiviridae*	*Alphatectivirus*

Funded by the European Union

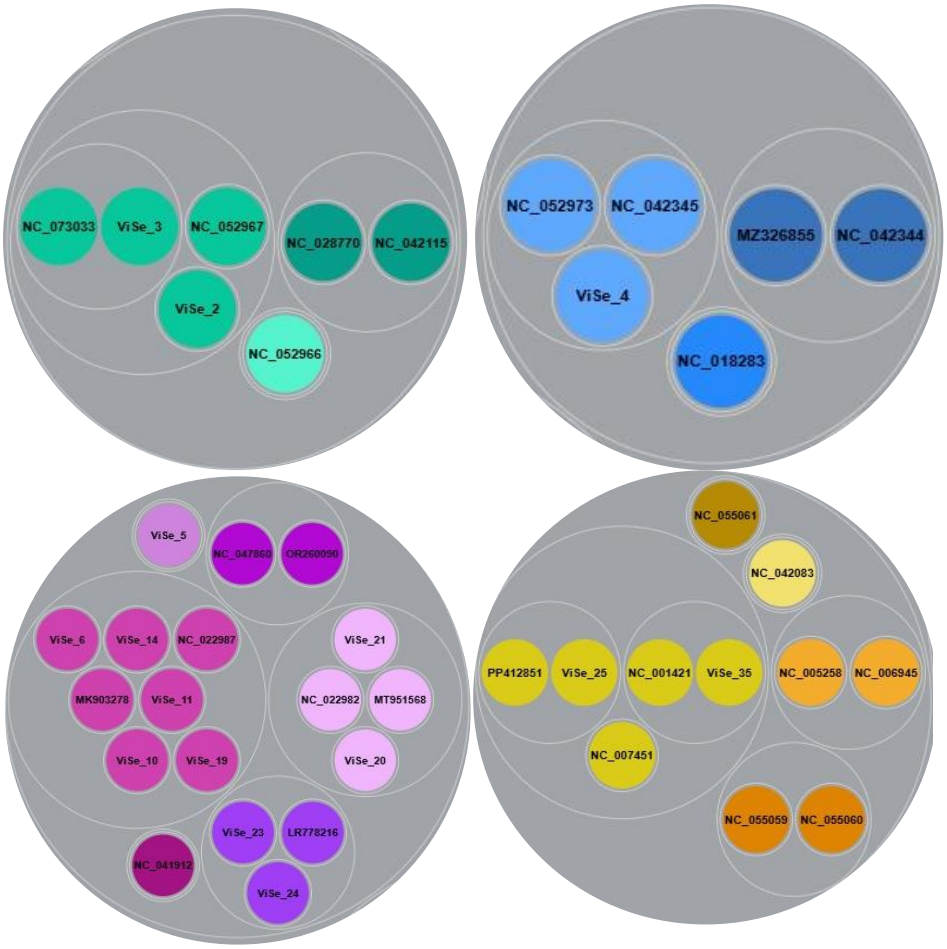


Figure 35: Circle packing of *the* VIRIDIC clustering based on intergenomic similarity. The outermost circles represent families: *Autographiviridae* (purple/pink), *Schitoviridae* (green), *Mesyanzhinovviridae* (turquoise), *Casjensviridae* (blue) and *Tectiviridae* (orange). The inner circles indicate clustering thresholds, with the innermost representing the 95% similarity threshold for species demarcation and the outermost representing the 68% threshold for genus classification. Representative phages are shown along with closely related published phage species and genera.

Additionally, transmission electron micrographs (TEM) revealed three main phage morphologies (Figure 36): a Sipho-type morphology, with isometric heads and noncontractile tails; ViSe_4 possessed a longer tail compared to phage ViSe_2, which had an average tail length of 141 nm. Notably, instead of the classical icosahedral capsid morphology, phage ViSe_2 displayed a prolate head structure. Phages ViSe_6 to ViSe_18, ViSe_21 and ViSe_22 exhibited a Podo-type morphology, with isometric heads and short stubby tails. The rest of phages displayed icosahedric capsids with a pseudo T=25 symmetry and an enclosed inner membrane vesicle.

Funded by
the European Union

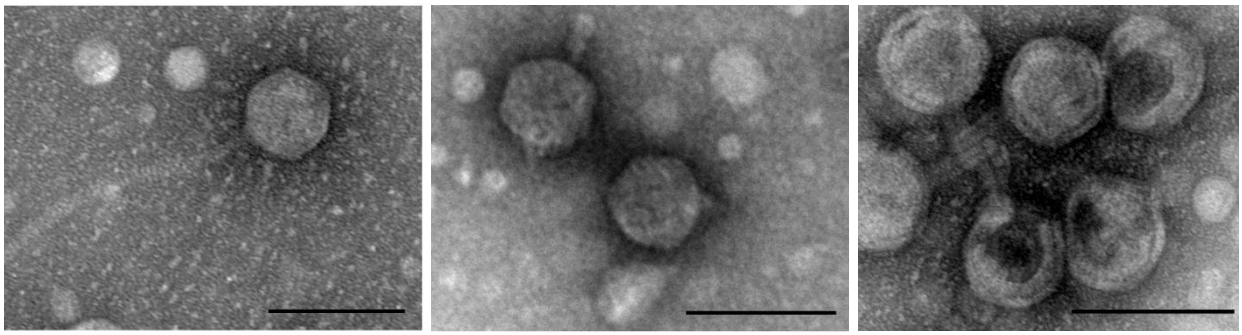


Figure 36: Transmission electron micrographs of three different morphotypes identified in the isolated phages: a Sipho-type morphology (left); a Podo-type morphology (center); and a pseudo T=25 symmetry with an enclosed inner membrane vesicle (right). Scale bar = 100 nm.

An in-house pipeline was developed to detect prophage genomes integrated in the *X. fastidiosa* strains. Additionally, the genomic analysis of a collection of 89 *X. fastidiosa* genomes was performed (Figure 36). In total, the diversity and distribution of prophages was studied across 89 *X. fastidiosa* strains representing the three main subspecies: *fastidiosa*, *multiplex* and *pauca*, as well as the two proposed subsp. *sandyi* and *morus,* representative of 28 sequence types (ST). A total of 527 intact prophages were identified, with a notable prevalence in strains of the subsp. *sandyi* and *multiplex*. Comparative analyses revealed 130 unique prophages, highlighting their role in enhancing genetic diversity through horizontal gene transfer and recombination. While some prophages were strain-specific, others were shared across multiple strains of the same subspecies or ST, suggesting clonal propagation (Figure 37). Genomic and phylogenetic comparisons showed clear distinctions between prophages and lytic phages and highlighted similarities among prophages from different subspecies, reflecting shared evolutionary processes. These findings will support future studies on the functional roles of specific prophage genes, their contributions to *X. fastidiosa* virulence and host range, and their potential applications in phage-based biocontrol.

An experimental directed evolution assay for optimization of phages from the collection that had slight activity against *X. fastidiosa* subsp. *multiplex* strains has been performed to increase efficacy. So far, no apparently significant changes have been observed in the evolved phages.

Finally, a collection of bacteriophages available in P8-INRAE was tested against *X. fastidiosa*, but none of them demonstrated robust efficacy. To circumvent this problem and identify potential new bacteriophages, plant material was sampled in Corsica in 2024 for new virus isolations, but no phages have been isolated.

Funded by the European Union

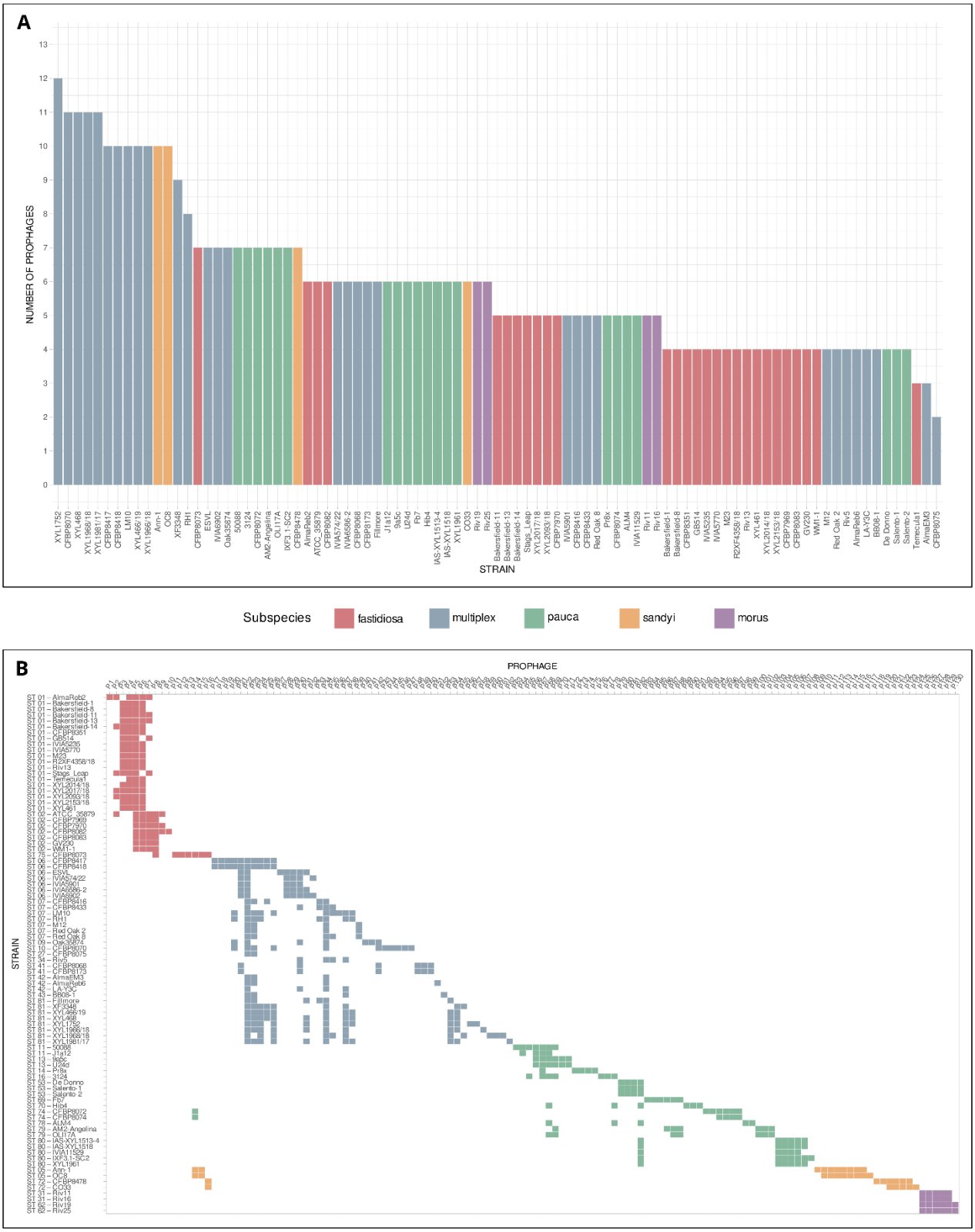


Figure 37: (**A**) Number of prophages predicted in Phastest for each strain of *Xylella fastidiosa*. (**B**) Infectivity matrix of the 130 obtained prophages with respect to the 89 strains where they were found. The colors indicate the subspecies of the strain: subsp. *fastidiosa* (light grey), *multiplex* (diagonal stripes), *pauca* (dotted), *sandy* (black) or *morus* (grey).

Funded by the European Union

2.4.2. Phage host range

The host range of the isolated phages was assessed using serial dilution spot assays against more than 10 bacterial isolates, including phytopathogenic *Xanthomonas* spp. strains and *X. fastidiosa* isolates. The phages displayed lytic activity against some *Xanthomonas* spp. and *X. fastidiosa* subsp. *fastidiosa* strains, with variability in the range and intensity depending on the phage. Most phages isolated from *Xanthomonas* spp. were capable of infecting strains IVIA 4165.15 of *X. arboricola* pv. *pruni*, XCC176 of *X. citri* subsp. *citri*, and CFBP 2523 of *X. albilineans*, excluding most phages from the *Tectiviridae* family. In contrast, other phytopathogenic strains such as IVIA 4928 of *X. euvesicatoria*, CFBP 2528 of *X. arboricola* pv. *juglandis* and XOO 93 of *Xanthomonas oryzae* pv. *oryzae* were susceptible only to specific phages. Notably, the strain CECT 914 of *X. phaseoli* was exclusively susceptible to phages from the *Tectiviridae* family. For *X. fastidiosa* subsp. *fastidiosa*, mainly strains ST1 were susceptible to the isolated phages. Among ST1 strains, most phages demonstrated consistent infectivity across isolates from Spain (IVIA 5770, IVIA 376.1/23, IVIA 906/24) and the strain Temecula from USA.

Bacterial susceptibility to phages was further analyzed by evaluating bacterial growth in liquid medium in the presence and absence of each phage at two concentrations (10^{10} and 10^{8} PFU/mL). Despite the variability observed among the *X. fastidiosa* subsp. *fastidiosa* ST1 strains, certain phages exhibited consistent and notable effects, which allowed their categorization according to their inhibitory potential and dose-dependent behavior. Phages that consistently and completely inhibited all tested strains were those finally selected (Figure 38): vB_Xf_IVIA-DoCa19, ViSe_2, ViSe_4, ViSe_6, ViSe_7, ViSe_8, ViSe_9, ViSe_10, ViSe_14, ViSe_15, ViSe_17, ViSe_18, ViSe_21, ViSe_22, ViSe_33, and ViSe_34.

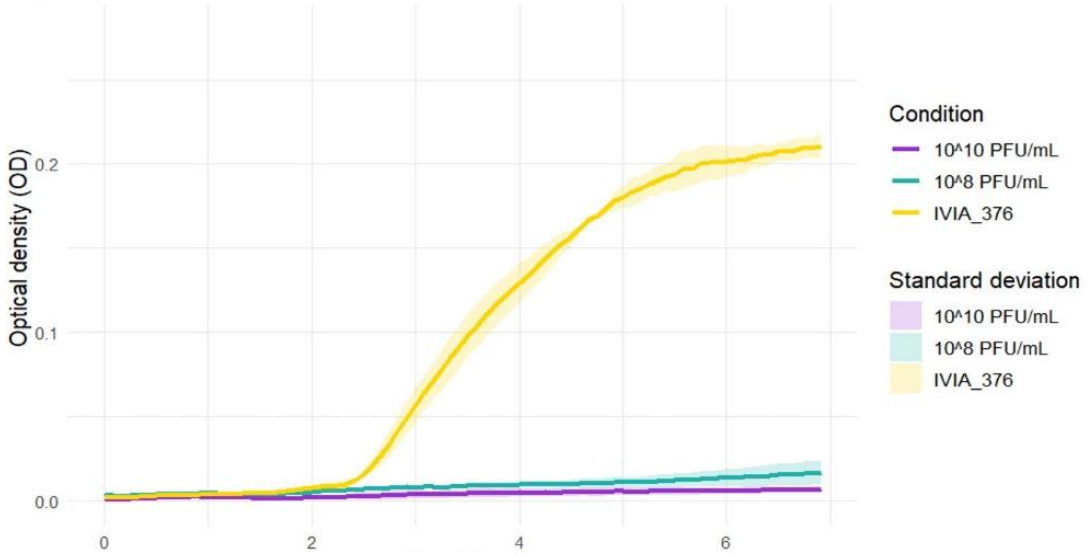


Figure 38: Growth curve of *Xylella fastidiosa* IVIA 376/23 strain in the presence and absence of one novel lytic phage (ViSe_2) throughout 7 days (measurements recorded every 2). Yellow color represents bacterial growth in the absence of phages, while purple and blue indicate the bacterial growth in the presence of phages at concentration of 10^{10} and 10^{8} PFU/mL, respectively. All experiments were performed in triplicate, with error bars representing the standard deviation.

Funded by the European Union

2.4.3. Screening *in planta* of selected bacteriophages

The effect of the phage vB_Xf_IVIA-DoCa19 was assayed in tobacco and periwinkle plants. In tobacco plants, the roots and the tissue at 5 and 10 cm above the inoculation point, *X. fastidiosa* IVIA 5770 strain was detected in the three replicates of control plants inoculated only with the bacterial strain; however, in the phage-treated plants, *X. fastidiosa* was only detected in some of them, in very low populations, between 7 (when phage was administered at the same time as IVIA 5770) and more than 40-50 (when the phage was administered after or before IVIA 5770) times lower than in the controls. As for the re-isolation, *X. fastidiosa* strain was easily re-isolated from all the plants used as positive controls, and from the two areas above the inoculation point and from the roots, while of the plants treated with the phage, *X. fastidiosa* was re-isolated from only from only one third of the inoculated plants, and in much lower number of colonies than in the positive controls. No symptoms related to X. fastidiosa were observed on either the positive controls or on any of the plants throughout the 4-month trial.

In periwinkle plants, vB_Xf_IVIA-DoCa19 and a cocktail of the phages vB_Xf_IVIA-DoCa15, vB_Xf_IVIA-DoCa18, vB_Xf_IVIA-DoCa19 and vB_Xf_IVIA-DoCa21 were assayed. After 4 month post-challenge, symptoms were observed after inoculation of strain IVIA 5770. To assess levels of symptomatology, we refer to the following scale: 0, no symptoms; 1, mild symptoms (isolated leaves show yellowing); 2, severe symptoms (more than 50% of leaves show yellowing) (Figure 39). At time four months, plants used as positive controls, inoculated only with the *X. fastidiosa* strain but no phages, showed symptoms of chlorosis and some wilting in most leaves, a level 2 of symptomatology. In contrast, challenged periwinkle plants treated with phage vB_Xf_IVIA-DoCa19 or the phage cocktail (treatment 1) showed no symptoms at all (level 0) or only mild symptoms (level 1). Moreover, internally, at the crown level, extensive necrosis of the vascular vessels was observed in the positive control plants, while in the phage-treated plants, vessels appear normal, like those of the negative control plants. Plants challenged with phages before (treatment 2) or after (treatment 3) inoculation with *X. fastidiosa* strain also showed no external symptoms, and only partial necrosis was observed in the vascular vessels of plants subjected to treatment 2.

A Taqman qPCR protocol was developed for detection and quantification of selected phages in planta. Results indicated that high phage concentrations were detected in most treated plants at 5 cm from the inoculation point, finding the lowest amount in plants treated with the phages at the same time as IVIA5770, and the highest one in plants treated with the cocktail 24 h after the bacterial inoculation.

Funded by the European Union

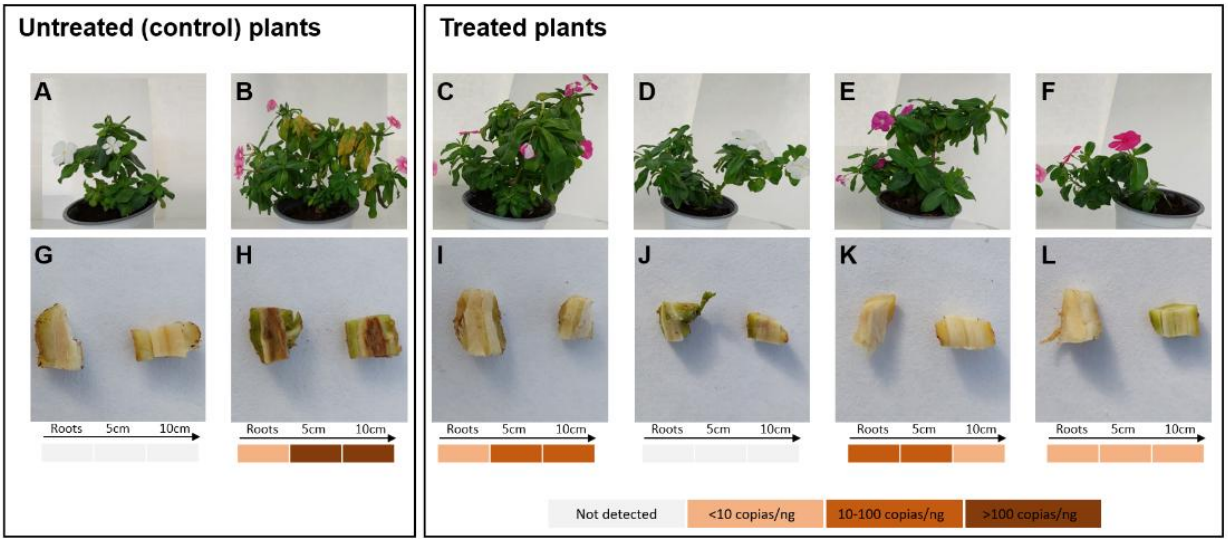


Figure 39: Periwinkle plants treated with a cocktail of the phages vB_Xf_IVIA-DoCa15, vB_Xf_IVIA-DoCa18, vB_Xf_IVIA-DoCa19 and vB_Xf_IVIA-DoCa21 (C,D, E, I, J, K) or only with the phage vB_Xf_IVIA-DoCa19 (F, L) at the same time (C, I, F, L), before (D, J), or after (E, K) of the inoculation of strain IVIA 5770 of *X. fastidiosa* subsp. *fastidiosa* ST1. Plants inoculated only with IVIA 5770 strain (B) or not inoculated with this strain (A) were used as positive and negative controls, respectively. The lower row of pictures shows the appearance of the xylem vessels in longitudinal sections of the stems. The heatmap represents the quantification of Xylella fastidiosa by qPCR (Harper et al., 2010, erratum 2013). Results were monitored 4 months after challenge.

In collaboration with the company 'Evolving Therapeutics SL', a promising phage with in vitro and in vivo activity tested against *X. fastidiosa* subsp. *fastidiosa* was used to perform a pilot trial in a grapevine field plot with high incidence of Pierce's disease in the Balearic Islands (Figure 40). The phage treatment was applied as preventive on healthy plants as well as a therapeutic on infected plants, to validate the use of phages in biocontrol of Pierce's disease in the field. The results, still under evaluation, show that when the phage was used as a preventative, healthy plants did not develop Pierce's disease symptoms and when used as a curative the symptoms did not evolve.

Funded by
the European Union



Figure 40: Researchers from Evolving Therapeutics performing a phage treatment on *Xylella fastidiosa* infected grapevines affected by Pierce's disease in Mallorca (Balearic Islands).

3. CONCLUSIONS

The main conclusions achieve from results presented in this deliverable are the following:

- Antimicrobial glasses and glass-ceramics were not enough active against *X. fastidiosa* in vitro.
- From the antimicrobial plant extracts, the olive extracts with the highest bactericidal effect was the extract enriched in Hydroxytyrosol (HT). In the case of Eucalyptus essential oil there was a strong antibacterial and bactericidal activity *in vitro* by a lytic mechanism, as well as a significant control of infections in almond, due to both activity against X. fastidiosa and elicitation of defense responses in the plant.
- From around 35 single synthetic peptides studied for its antibacterial, bactericidal, antibiofilm, antiLPS, antimotility, phytotoxicity and hemolytic activity, a set of five (BP178, BP100, HH15, 1036, FV7) showed significantly high inhibition of *X. fastidiosa* infections in *N. benthamiana* and almond. The mechanisms of action were very diverse and specific. For example, BP178 was bactericidal and elicitor of plant defense, BP100 was motility inhibitor, FV7 and HH15 only defense elicitor. However, all of them were effective in inhibiting infections at different levels.

Funded by the European Union

- We have generated a diverse collection of phages with 19 being selected due to their lytic activity against *X. fastidiosa*. The pilot scale-up conducted in the field with one of them has been successful in terms of symptom reduction in *X. fastidiosa*-infected grapevines. The phage collection is an important resource for evaluating phage interactions for cocktail production and for using the directed evolution tool to fine-tune conditions, all with the goal of optimizing this biocontrol strategy.

4. PUBLICATIONS FROM THIS DELIVERABLE

4.1. Articles published

Baro A, Saldarelli P, Saponari M, Montesinos E and Montesinos L (2022). *Nicotiana benthamiana* as a model plant host for *Xylella fastidiosa*: Control of infections by transient expression and endotherapy with a bifunctional peptide. **Front. Plant Sci**. 13:1061463. doi: 10.3389/fpls.2022.1061463.

Moll L, Baró A, Montesinos L, Badosa E, Bonaterra A, Montesinos E. (2022). Induction of Defense Responses and Protection of Almond Plants Against *Xylella fastidiosa* by Endotherapy with a Bifunctional Peptide. **Phytopathology** 112:1907-1916. doi: 10.1094/PHYTO-12-21-0525-R. Epub 2022 Aug 8.

Montesinos L, Baró A, Gascón B and Montesinos E (2023). Bactericidal and plant defense elicitation activities of *Eucalyptus* oil decrease the severity of infections by *Xylella fastidiosa* on almond plants. **Front. Plant Sci.** 14:1122218. doi: 10.3389/fpls.2023.1122218.

Montesinos E. (2023). Functional Peptides for Plant Disease Control. **Annu. Rev. Phytopathol**. 61:301–24. doi:10.1146/annurev-phyto-021722-034312.

Moll, L., Giralt, N., Planas, M. et al. (2024). *Prunus dulcis* response to novel defense elicitor peptides and control of *Xylella fastidiosa* infections. **Plant Cell Rep** 43:190. doi:10.1007/s00299-024-03276-x.

Moll., L., Badosa, E., De la Fuente, L., Montesinos, E., Plansa, M., Bonaterra, A., Feliu, L. (2025). Mitigation of Almond Leaf Scorch by a Peptide that Inhibits the Motility of *Xylella fastidiosa*. **Plant Dis.** 109:327-340. doi:10.1094/PDIS-07-24-1414-RE.

4.2. Articles in preparation or under revision

Domingo-Calap, M.L., Bernabéu-Gimeno; M., Simó-Esquivel, M., Morán, F., Aure, C.M., Navarro-Herrero, I., Domingo-Calap, P., Marco-Noales, E. (2025). Phage biocontrol against the phytopathogenic bacterium *Xylella fastidiosa*. In preparation.

Sellés-Ribera, C., Marco-Noales, E., Domingo-Calap, P. (2025). Diversity and lytic potential of novel phages targeting *Xylella fastidiosa* subsp. *fastidiosa*, the causal agent of Pierce's disease of grapevines.

Funded by the European Union

Tomás-Tomás, M., Velasco-Amo, M.P., Arias-Giraldo, L.F., Marco-Noales, E., Landa, B.B., Domingo-Calap, P. (2025). Genomic analysis of prophage distribution in *Xylella fastidiosa* reveals extensive diversity and horizontal gene transfer. Phytopathology (Under revision).

5. REFERENCES

Amanifar, N., Taghavi, M., and Salehi, M. (2016). *Xylella fastidiosa* from almond in Iran: overwinter recovery and effects of antibiotics. *Phytopathol. Mediterr.* 55, 337–345. doi:10.14601/Phytopathol_Mediterr-17682.

Anguita-Maeso, M., Ares-Yebra, A., Haro, C., Román-Écija, M., Olivares-García, C., Costa, J., et al. (2022). *Xylella fastidiosa* infection reshapes microbial composition and network associations in the xylem of almond trees. *Front. Microbiol.* 13. doi:10.3389/fmicb.2022.866085.

Baccari, C., Antonova, E., and Lindow, S. (2019). Biological control of Pierce's disease of grape by an endophytic bacterium. *Phytopathology®* 109, 248–256. doi:10.1094/PHYTO-07-18-0245-FI.

Baró, A., Mora, I., Montesinos, L., and Montesinos, E. 2020. Differential susceptibility of *Xylella fastidiosa* strains to synthetic bactericidal peptides. Phytopathology 110:1018–1026.

Baró, A., Saldarelli, P., Saponari, M., Montesinos, E., and Montesinos, L. (2022). *Nicotiana benthamiana* as a model plant host for *Xylella fastidiosa*: Control of infections by transient expression and endotherapy with a bifunctional peptide. *Front. Plant Sci.* 13. doi:10.3389/fpls.2022.1061463.

Bruno, G. L., Cariddi, C., and Botrugno, L. (2021). Exploring a sustainable solution to control *Xylella fastidiosa* subsp. *pauca* on olive in the Salento Peninsula, Southern Italy. *Crop Prot.* 139, 105288. doi:10.1016/j.cropro.2020.105288.

Burbank, L. P. (2022). Threat of *Xylella fastidiosa* and options for mitigation in infected plants. *CABI Rev.* doi:10.1079/cabireviews202217021.

Cabal, B., Alou, L., Cafini, F., Couceiro, R., Sevillano, D., Esteban-Tejeda, L., Guitián, F., Torrecillas, R., and Moya, J. S. (2014). A new biocompatible and antibacterial phosphate free glass-ceramic for medical applications. Scientific Reports 4:5440.

Das, M., Bhowmick, T. S., Ahern, S. J., Young, R., and Gonzalez, C. F. (2015). Control of Pierce's Disease by phage. *PLoS One* 10, 1–15. doi:10.1371/journal.pone.0128902.

Davis, M. J., French, W. J., and Schaad, N. W. (1981). Axenic culture of the bacteria associated with phony disease of peach and plum leaf scald. *Curr. Microbiol*. 6:309-314.

Deyett, E., and Rolshausen, P. E. (2019). Temporal dynamics of the sap microbiome of grapevine under high Pierce's disease pressure. *Front. Plant Sci.* 10. doi:10.3389/fpls.2019.01246.

Domingo-Calap, M. L., Aure Cristina, M., Navarro-Herrero, I., Simó-Esquivel, M., Biosca Elena, G., Román-Écija, M., et al. (2021). Pathogenicity of *Xylella fastidiosa* subsp. *multiplex* isolates from Alicante outbreak (mainland Spain) on different hosts. *3rd Eur. Conf. Xylella*

Funded by the European Union

fastidiosa XF-ACTORS Final Meet. doi:10.5281/zenodo.4678347.

Dourado, M. N., Pierry, P. M., Feitosa-Junior, O. R., Uceda-Campos, G., Barbosa, D., Zaini, P. A., et al. (2023). Transcriptome and secretome analyses of endophyte Methylobacterium mesophilicum and pathogen *Xylella fastidiosa* interacting show nutrient competition. *Microorganisms* 11, 2755. doi:10.3390/microorganisms11112755.

EFSA PLH Panel (2018). Updated pest categorisation of Xylella fastidiosa. *EFSA J.* 16. doi:10.2903/j.efsa.2018.5357.

EFSA PLH Panel (2019). Effectiveness of in planta control measures for Xylella fastidiosa. *EFSA J.* 17. doi:10.2903/j.efsa.2019.5666.

Esteban-Tejeda, L., Prado, C., Cabal, B., Sanz, J., Torrecillas, R., and Moya, J. S. 2015. Antibacterial and antifungal activity of ZnO containing glasses. PLoS One 10:e0132709.

Fernández-Bolaños, J., Rodríguez, G., Senent Rubio, F., Lama-Muñoz, A., Fernández-Bolaños, J.M., Maya, I., and López, O. 2013. Method for obtaining Hydroxytyrosol extract, mixture of Hydroxytyrosol and 3,4-dihydroxyphenylglycol extract, and Hydroxytyrosyl acetate extract from by-products of the olive tree and the purification of thereof. International patent (17/01/2013) N: WO 2013/007850A1. In explotation by S.V.M. S.L. company.

Foix, L., Nadal, A., Zagorščak, M., Ramšak, Ž., Esteve-Codina, A., Gruden, K., et al. (2021). Prunus persica plant endogenous peptides PpPep1 and PpPep2 cause PTI-like transcriptome reprogramming in peach and enhance resistance to Xanthomonas arboricola pv. pruni. *BMC Genomics* 22, 360. doi:10.1186/s12864-021-07571-9.

Ge, Q., Cobine, P. A., and de la Fuente, L. (2020). Copper supplementation in watering solution reaches the xylem but does not protect tobacco plants against *Xylella fastidiosa* infection. *Plant Dis.* 104, 724–730. doi:10.1094/PDIS-08-19-1748-RE.

Giampetruzzi, A., Baptista, P., Morelli, M., Cameirão, C., Lino Neto, T., Costa, D., et al. (2020). Differences in the endophytic microbiome of olive cultivars infected by *Xylella fastidiosa* across seasons. *Pathogens* 9, 723. doi:10.3390/pathogens9090723.

Lenth, R., Singmann, H., Love, J., Buerkner, P., and Herve, M. 2019. R Package emmeans. *CRAN.* https://CRAN. R-project. org/package= emmeans (accessed May 21, 2025).

Lindow, S., Koutsoukis, R., Meyer, K., and Baccari, C. (2024). Control of Pierce's Disease of grape with Paraburkholderia phytofirmans PsJN in the field. *Phytopathology®* 114, 503–511. doi:10.1094/PHYTO-06-23-0219-R.

Marelli, L., Trane, M., Barbero Vignola, G., Gastaldi, C., Guerreiro, M. M., Delgado Callico, L., et al. (2025). *Delivering the EU Green Deal – Progress towards targets*. Publications Office of the European Union doi:doi/10.2760/3105205.

Meyer, M. M., and Kirkpatrick, B. C. (2011). Exogenous applications of abscisic acid increase curing of Pierce's disease-affected grapevines growing in pots. *Plant Dis.* 95, 173–177. doi:10.1094/PDIS-06-10-0446.

Moll, L. (2024). Synthetic peptides that target key processes of *Xylella fastidiosa* and its host for the leaf scorch control in almond plants. Available at: http://hdl.handle.net/10803/693647.

Moll, L., Badosa, E., Planas, M., Feliu, L., Montesinos, E., and Bonaterra, A. (2021).

Funded by the European Union

Antimicrobial peptides with antibiofilm activity against *Xylella fastidiosa*. *Front. Microbiol.* 12, 1–16. doi:10.3389/fmicb.2021.753874.

Morelli, M., García-Madero, J. M., Jos, Á., Saldarelli, P., Dongiovanni, C., Kovacova, M., et al. (2021). *Xylella fastidiosa* in olive: a review of control attempts and current management. *Microorganisms* 9, 1771. doi:10.3390/microorganisms9081771.

Navarrete, F., and De La Fuente, L. (2014). Response of *Xylella fastidiosa* to zinc: Decreased culturability, increased exopolysaccharide production, and formation of resilient biofilms under flow conditions. *Appl. Environ. Microbiol.* 80, 1097–1107. doi:10.1128/AEM.02998-13.

Picchi, S. C., Rebelatto, D., Martins, P. M. M., Blumer, S., Mesquita, G. L., Hippler, F. W. R., et al. (2024). N -acetylcysteine absorption and its potential dual effect improve fitness and fruit yield in Xylella fastidiosa infected plants. *Pest Manag. Sci.* doi:10.1002/ps.8137.

Rodríguez-Gutiérrez, G., Fernández-Bolaños, J., Bermúdez-Oria, A., Fernández-Prior, M.A., and Espejo-Calvo, J.A. Procedure for obtaining 3,4-dihydroxymethylglycol (DHFG). P202030495 (28 May 2020).

Scortichini, M., Chen, J., de Caroli, M., and Dalessandro, G. (2018). A zinc, copper and citric acid biocomplex shows promise for control of *Xylella fastidiosa* subsp. *pauca* in olive trees in Apulia region (southern Italy). *Phytopathol. Mediterr.* 57, 48–72. doi:10.14601/Phytopathol_Mediterr-21985.

Stefani, E., Obradović, A., Gašić, K., Altin, I., Nagy, I. K., and Kovács, T. (2021). Bacteriophage-mediated control of phytopathogenic Xanthomonads: a promising green solution for the future. *Microorganisms* 9, 1056. doi:10.3390/microorganisms9051056.

Tataridas, A., Kanatas, P., Chatzigeorgiou, A., Zannopoulos, S., and Travlos, I. (2022). Sustainable crop and weed management in the era of the EU Green Deal: a survival guide. *Agronomy* 12, 589. doi:10.3390/agronomy12030589.

Tatulli, G., Baldassarre, F., Schiavi, D., Tacconi, S., Cognigni, F., Costantini, F., et al. (2024). Chitosan-coated fosetyl-Al nanocrystals' efficacy on *Nicotiana tabacum* colonized by *Xylella fastidiosa*. *Phytopathology®* 114, 1466–1479. doi:10.1094/PHYTO-04-24-0144-R.

Tatulli, G., Modesti, V., Pucci, N., Scala, V., L'aurora, A., Lucchesi, S., et al. (2021). Further in vitro assessment and mid-term evaluation of control strategy of *Xylella fastidiosa* subsp. pauca in olive groves of Salento (Apulia, Italy). *Pathogens* 10, 85. doi:10.3390/pathogens10010085.

Vergine, M., Meyer, J. B., Cardinale, M., Sabella, E., Hartmann, M., Cherubini, P., et al. (2019). The *Xylella fastidiosa*-resistant olive cultivar "Leccino" has stable endophytic microbiota during the Olive Quick Decline Syndrome (OQDS). *Pathogens* 9, 35. doi:10.3390/pathogens9010035.

Zhang, S., Jain, M., Fleites, L. A., Rayside, P. A., and Gabriel, D. W. (2019). Identification and characterization of menadione and benzethonium chloride as potential treatments of Pierce's disease of grapevines. *Phytopathology* 109, 233–239. doi:10.1094/PHYTO-07-18-0244-FI.

Funded by the European Union

Wells, J.M., Raju, B.C., Nyland, G., and Lowe, S.K. (1981). Medium for isolation and growth of bacteria associated with plum leaf scald and phony peach diseases. *Appl. and Environ. Microbiol.* 42:357–363

Funded by
the European Union